Cutoff Rate Performance of Memoryless Modulation Schemes Operating on Slow-Fading Rician Channels †

Kyuhyoun Park and James W. Modestino
Electrical, Computer and Systems Engineering Department
and Department of Engineering Science
Rensselaer Polytechnic Institute
Troy, New York 12180

October 10, 1995

Abstract

This paper provides a comprehensive information-theoretic characterization of the slow-fading Rician channel, based on the channel cutoff rate, to allow prediction and assessment of modulation/coding tradeoffs as a function of channel parameters and specific system implementation details. Our approach is to first develop maximum-likelihood (ML) receiver implementations for various cases of when *perfect* or *no* channel state information (CSI) is available, and when either *ideal* or *no* interleaving/deinterleaving strategies are used. The cutoff rate is then evaluated, by straightforward Chernoff bounding techniques, for the coding channel resulting from the use of the optimum demodulator which computes the corresponding ML decoding metrics. More specifically, we derive Chernoff bounds on the pairwise codeword error probability which are then used to provide explicit evaluation of the cutoff rate for selected memoryless modulation schemes for the various channel conditions and system implementation details considered. While some of the results described here have been developed previously as special cases, and generally under more restrictive assumptions, the unified and comprehensive nature of the present work should provide a more complete perspective useful in assessing potential modulation/coding tradeoffs on representative fading channels.

†This work was supported in part by ARPA under Contract No. F30602-92-C-0030. and in part by DAAH04-95-1-0103 (Laboratory for Information and Decision Systems, Massachusetts Institute of Technology)

I. INTRODUCTION:

The performance/complexity characterization of coded communication systems operating over slowly-fading channels has been an area of interest to researchers for many years. As first argued by Massey [7] in the case of the AWGN channel, the channel cutoff rate, R_0, can provide a useful tool in assessing the performance/complexity tradeoffs associated with the design and implementation of modulation/coding systems. The cutoff rate has since proven its usefulness as a rational and effective tool for assessing modulation/coding tradeoffs on a variety of real-world physical channels and for providing practical bounds on throughputs for which reliable communication is possible with appropriately chosen coding schemes of reasonable and acceptable complexity. In this work we provide a systematic and comprehensive evaluation of the channel cutoff rate for the slow-fading Rician channel for selected memoryless modulation schemes and under a variety of assumptions on system implementation details. This work complements and extends previous results [14],[18] on evaluation of the cutoff rate for the specific case of MPSK modulation on the slow-fading Rician channel when *perfect* channel state information (CSI) is available. It is hoped that the unified and comprehensive treatment provided here will provide a more useful overall perspective in assessing modulation/coding tradeoffs under a variety of channel conditions and assumptions on system implementation details.

More specifically, this paper provides explicit development and numerical evaluation of the cutoff rate of *memoryless* modulation schemes for the slow-fading Rician channel not only when *perfect* CSI is available, but also when CSI is *not* available. Furthermore, both cases are considered under different assumptions on the interleaving/deinterleaving strategy employed. We characterize the performance of a *memoryless* modulation scheme operating on the slow-fading Rician channel by first developing maximum-likelihood (ML) receivers for the various cases of when *perfect* or *no* CSI is available and when either *ideal* or *no* interleaving/deinterleaving strategies are used. If *perfect* estimates of the fading components could be obtained, then it is clear that the only random component is the additive noise and then the ML decoding metric in this case is simply the sum of the individual *branch* metrics whether or not interleaving/deinterleaving is used. On the other hand, if CSI is not available ML decoding is quite complicated. Fortunately, for constant-envelope modulation

schemes, the ML decoding rule again reduces to the sum of the individual *branch* metrics provided a differential encoding/decoding technique is employed. This modulation/coding technique is called M-ary differential phase shift-keyed modulation (MDPSK). When the ML decoding metric can be expressed as the sum of individual *branch* metrics, such as for memoryless modulation with *perfect* CSI or for MDPSK with differential detection, the ML metric is not affected by using interleaving/deinterleaving. However, the channel resulting from use of *ideal* interleaving/deinterleaving results in *uncorrelated* fading amplitudes and this generally improves the performance of the *memoryless* modulation scheme since the decoder corresponding to the channel encoder will be able to provide *random* error-correction *even* in the presence of deep fades [1],[12],[13]. Therefore, for memoryless modulation schemes with *perfect* CSI or MDPSK with *no* CSI, performance can be expected to be improved by using *ideal* interleaving/deinterleaving.

Having developed appropriate ML receiver implementations, we derive Chernoff upper bounds on the pairwise error probability for the various cases considered which in turn allow explicit evaluation of the cutoff rate for several different modulation schemes operating on the slow-fading Rician channel. For the case of *ideal* interleaving/deinterleaving, we also consider the limiting cutoff rate performance when the restriction of a fixed finite alphabet size, M, is removed such that $M \rightarrow \infty$.

The remainder of this paper is organized as follows: In Section II, we describe some technical preliminaries, including our modeling assumptions and other system details. In Section III, we provide the ML decoding rules for the memoryless modulation schemes under consideration when *perfect* or *no* CSI is available. With these ML receivers designed for the different cases of *perfect* and *no* CSI, we then develop in Section IV explicit cutoff rate results for *memoryless* modulation schemes with finite alphabet size M operating on slow-fading Rician channels. In Section V we also provide limiting cutoff rate results for selected modulation schemes when the restriction of a fixed finite alphabet size, M, is removed. We then provide numerical results in Section VI as well as a discussion of the use of these cutoff rate results for system design. Finally, a summary and conclusions can be found in Section VII.

II. PRELIMINARIES:

We assume that the received signal can be expressed in complex envelope notation as

$$r(t) = \sqrt{2}Re\{\tilde{r}(t)e^{j2\pi f_0 t}\}, \tag{1}$$

where f_0 is the carrier frequency and $\tilde{r}(t)$ is the *complex envelope* of the received signal. It can be expressed as[1]

$$\tilde{r}(t) = \tilde{z}(t)\tilde{s}(t;\mathbf{c}) + \tilde{n}(t), \tag{2}$$

with $\tilde{s}(t;\mathbf{c})$ the complex envelope of the transmitted signal, $\mathbf{c} = (\cdots, c_{-1}, c_0, c_1, \cdots)$ the M-ary signal sequence to be transmitted, $\tilde{n}(t)$ a complex zero-mean additive white Gaussian noise (AWGN) process whose inphase and quadrature (I/Q) components each process double-sided noise spectral density $N_0/2$ watts/Hz and, finally, $\tilde{z}(t)$ is a complex fading process. Here, the fading component is assumed of the form

$$\tilde{z}(t) = \Gamma e^{j\psi} + \tilde{a}(t), \tag{3}$$

where Γ is the amplitude of the *specular* component, ψ is a random phase uniformly distributed on $[0, 2\pi]$ and $\tilde{a}(t)$ is a complex zero-mean Gaussian noise process with covariance function

$$R_a(\tau) = E\{\tilde{a}(t)\tilde{a}^*(t+\tau)\}, \tag{4}$$

representing the *diffuse* fading component. We will assume that $\tilde{a}(t)$ has independent I/Q components each processing variance σ_a^2. The ratio of specular-to-diffuse energy is then $\zeta^2 = \Gamma^2/2\sigma_a^2$ where we furthermore assume $\Gamma^2 + 2\sigma_a^2 = 1$, representing a power conservation constraint.

To simplify, we assume that the fading is sufficiently slow so that the amplitude and phase perturbations may be considered constant throughout any signaling interval of duration T_s such that

$$\tilde{z}(t) = \tilde{z}_i; \quad iT_s \le t < (i+1)T_s, \quad i = 0, \pm 1, \pm 2, \cdots. \tag{5}$$

We also assume knowledge of the phase ψ of the specular component and, without loss of generality, set it to zero. More specifically, we assume that

$$\tilde{z}_i = \Gamma + \tilde{a}_i; \quad i = 0, \pm 1, \pm 2, \cdots, \tag{6}$$

[1]We assume the channel has Doppler dispersion but no delay dispersion.

where $\tilde{a}_i$ is a complex first-order Gaussian autoregressive(AR) processes. That is, we assume that

$$\tilde{a}_i = \rho\tilde{a}_{i-1} + \sqrt{1-\rho^2}\tilde{w}_i; \quad i = 0, 1, 2, \cdots, \tag{7}$$

where $\tilde{w}_i$ is a complex zero-mean independent and identically distributed(i.i.d) Gaussian sequence whose I/Q components each have variance σ_a^2, and ρ is the serial correlation coefficient of the diffuse fading component. For example, in the case of the second-order Butterworth fading spectra, ρ can be expressed as [6]

$$\rho = \exp(-\sqrt{2}\pi B_0 T_s)(\cos(\sqrt{2}\pi B_0 T_s) + \sin(\sqrt{2}\pi B_0 T_s)), \tag{8}$$

where the dimensionless quantity B_0T_s is a measure of the Doppler spread normalized to the baud rate. Since, under the stated assumptions, $\tilde{\mathbf{z}}^N \triangleq (\tilde{z}_1, \tilde{z}_2, \cdots, \tilde{z}_N)$ is a first-order Gauss-Markov process, the probability density function (pdf) $p(\tilde{\mathbf{z}}^N)$ is then given by

$$p(\tilde{\mathbf{z}}^N) = \frac{1}{\pi^N|\mathbf{K}|}\exp\{- < (\tilde{\mathbf{z}}^N - \Gamma\mathbf{u}), \mathbf{K}^{-1}(\tilde{\mathbf{z}}^N - \Gamma\mathbf{u}) >\}, \tag{9}$$

where $\mathbf{u}$ is a unit vector all of whose elements are unity and $\mathbf{K}$ is the common covariance matrix associated with the I/Q components of the sequence $\{\tilde{a}_i\}$ given by

$$\mathbf{K} = 2\sigma_a^2 \begin{pmatrix} 1 & \rho & \cdots & \rho^{N-2} & \rho^{N-1} \\ \rho & 1 & \cdots & \rho^{N-3} & \rho^{N-2} \\ \vdots & \vdots & \ddots & \vdots & \vdots \\ \rho^{N-2} & \rho^{N-3} & \cdots & 1 & \rho \\ \rho^{N-1} & \rho^{N-2} & \cdots & \rho & 1 \end{pmatrix}. \tag{10}$$

Here we denote the complex inner product as $< \tilde{\mathbf{x}}, \tilde{\mathbf{y}} >= \tilde{\mathbf{x}}^\dagger\tilde{\mathbf{y}}$, where the dagger "†" represents complex conjugate transpose and the vectors are of arbitrary length. Assuming *ideal* interleaving/deinterleaving is available, the Markov chain which produces the channel memory is then randomized so that the fading components $\tilde{z}_i$ are i.i.d., and the amplitude or envelope process $|\tilde{z}_i|$ possesses the Rician pdf

$$\begin{aligned} p(|\tilde{z}_i|) &= \frac{|\tilde{z}_i|}{2\pi\sigma_a^2}\exp\Big\{-\frac{|\tilde{z}_i|^2 + \Gamma^2}{2\sigma_a^2}\Big\} I_0\Big(\frac{|\tilde{z}_i|\Gamma}{\sigma_a^2}\Big); \ |\tilde{z}_i| \geq 0, \\ &= 0; \quad |\tilde{z}_i| < 0, \end{aligned} \tag{11}$$

where $I_0(\cdot)$ is the modified Bessel function of the first kind of order zero.

We now assume that the demodulator produces the sequence of decision variables

$$\tilde{r}_i'(c_i) = \frac{1}{E_s}\int_{iT_s}^{(i+1)T_s} \tilde{r}(t)\tilde{s}^*(t;c_i)dt;\ i = 0, \pm 1, \pm 2, \cdots, \tag{12}$$

representing normalized conventional matched filter outputs. The normalization factor E_s is the average signal energy and can be expressed in terms of the transmitted signal in a period T_s as

$$\begin{aligned} E_s &\triangleq E\{\int_{iT_s}^{(i+1)T_s} |\tilde{s}(t;c_i)|^2 dt\} \\ &= E\{A^2(c_i)\}, \end{aligned} \tag{13}$$

where we make use of the representation

$$\tilde{s}(t;c_i) = A(c_i)e^{j\phi(c_i)}p(t - iT_s);\ iT_s \leq t < (i+1)T_s, \tag{14}$$

with $A(c_i)$ the amplitude of the signaling element in the ith signaling interval, $\phi(c_i)$ the corresponding phase and $p(t)$ a unit-energy pulse vanishing outside the interval $[0, T_s]$. We assume that all M signals are equally likely, and define the normalized complex amplitude of a signaling element as

$$\tilde{s}(c_i) = \frac{A(c_i)}{\sqrt{E_s}}e^{j\phi(c_i)}, \tag{15}$$

such that $E\{|\tilde{s}(c_i)|^2\} = 1$. Then the sequence of decision variables in (12) can be written as

$$\tilde{r}_i'(c_i) = \tilde{r}_i\tilde{s}^*(c_i);\ iT_s \leq t < (i+1)T_s, \tag{16}$$

where

$$\tilde{r}_i = \frac{1}{\sqrt{E_s}}\int_{iT_s}^{(i+1)T_s} \tilde{r}(t)p(t - iT_s)dt;\ i = 0, \pm 1, \pm 2, \cdots \tag{17}$$

is independent of the hypothesized symbol, c_i. Now $\tilde{r}_i$ can be expressed as

$$\tilde{r}_i = \tilde{z}_i\tilde{s}(c_i) + \tilde{n}_i, \tag{18}$$

where

$$\tilde{n}_i \triangleq \frac{1}{\sqrt{E_s}}\int_{iT_s}^{(i+1)T_s} \tilde{n}(t)p(t - iT_s)dt;\ i = 0, \pm 1, \pm 2, \cdots, \tag{19}$$

is an i.i.d. sequence of complex zero-mean Gaussian variables whose I/Q components each have variance $N_0/2E_s$. Note that $|\tilde{s}(c_i)|^2$ is unity for the case of constant-envelope signaling formats, such as MPSK, and the matched filter outputs are then simply expressed as

$$\tilde{r}_i = \tilde{z}_i e^{j2\pi c_i/M} + \tilde{n}_i. \tag{20}$$

III. Evaluation of maximum-likelihood (ML) Decoding Metrics:

The optimum receiver structure for detecting a known signal in some specified noise environment is generally based upon a threshold test on the likelihood functional. In this section we provide explicit evaluation of the likelihood functional in the special case of the slow-fading Rician channel. This is the situation, as described above, where the complex envelope of the fading process is constant over the signaling interval.

III.1. Memoryless Modulation with Perfect CSI

The likelihood functional for estimation of the transmitted sequence[2], $\mathbf{c}^N$, given *perfect* CSI, as represented by the channel state sequence, $\tilde{\mathbf{z}}^N$, is given by [16]

$$\Lambda\{\tilde{r}(t); \mathbf{c}^N, \tilde{\mathbf{z}}^N\} = \exp\Big\{\sum_{i=1}^{N}[Re\{\tilde{r}_i \tilde{z}_i^* \tilde{s}^*(c_i)\} - \frac{1}{2}|\tilde{s}(c_i)|^2|\tilde{z}_i|^2]\Big\}, \tag{21}$$

with $\tilde{r}_i$ representing the conventional matched-filter outputs in (17) and the sequel and $\tilde{s}(c_i)$ representing the normalized complex signaling element in (14). The ML estimate $\hat{\mathbf{c}}^N$ is obtained by maximizing this quantity over all possible $\mathbf{c}^N$. If *perfect* CSI is available, whether or not interleaving/deinterleaving is used, a decision rule *equivalent* to the ML decision rule is to choose the transmitted sequence $\mathbf{c}^N$ such that

$$\hat{\mathbf{c}}^N = \arg \max_{\mathbf{c}^N} m_{ML}(\tilde{\mathbf{r}}^N; \mathbf{c}^N, \tilde{\mathbf{z}}^N), \tag{22}$$

where $\tilde{\mathbf{r}}^N = (\tilde{r}_1, \tilde{r}_2, \cdots, \tilde{r}_N)$ represents the received matched filter output sequence and the decoding metric is given by

$$m_{ML}(\tilde{\mathbf{r}}^N; \mathbf{c}^N, \tilde{\mathbf{z}}^N) = \sum_{n=1}^{N} m_{ML}(\tilde{r}_i; c_i, \tilde{z}_i), \tag{23}$$

with the corresponding *branch metric*

$$m_{ML}(\tilde{r}_i; c_i, \tilde{z}_i) = Re\{\tilde{r}_i \tilde{z}_i^* \tilde{s}^*(c_i)\} - \frac{1}{2}|\tilde{s}(c_i)|^2|\tilde{z}_i|^2. \tag{24}$$

For constant-envelope modulation, $|\tilde{s}(c_i)|^2$ is unity for all i, and the second term on the right-hand side in (24) can be eliminated.

[2]Here, and throughout the remainder of this paper, the superscript indicates the finite length of a sequence.

III.2. Memoryless Modulation with No CSI

In the absence of CSI, we first consider the conditional pdf $p(\tilde{\mathbf{r}}^N|\mathbf{c}^N)$ for the demodulator channel output sequence $\tilde{\mathbf{r}}^N = (\tilde{r}_1, \tilde{r}_2, \ldots, \tilde{r}_N)$ described by (17) which can be expressed as

$$\tilde{\mathbf{r}}^N = \mathbf{S}\tilde{\mathbf{z}}^N + \tilde{\mathbf{n}}^N, \tag{25}$$

where $\mathbf{S}$ is a *diagonal* matrix with elements $\{\tilde{s}(c_i)\}$ given by (14) and $\tilde{\mathbf{n}}^N = (\tilde{n}_1, \tilde{n}_2, \cdots, \tilde{n}_N)$ is the noise sequence in (19). Then the conditional distribution of this sequence is given by

$$p(\tilde{\mathbf{r}}^N|\mathbf{c}^N) = \frac{1}{\pi^N|\mathbf{H}||\mathbf{B}|}\exp\left\{- < (\tilde{\mathbf{r}}^N - \Gamma e^{j\psi}\mathbf{Su}), (\mathbf{SHS}^\dagger)^{-1}(\tilde{\mathbf{r}}^N - \Gamma e^{j\psi}\mathbf{Su}) >\right\}, \tag{26}$$

with

$$\mathbf{H} = \mathbf{K} + (N_0/E_s)\mathbf{B}^{-1}, \tag{27}$$

where $\mathbf{B}(= \mathbf{SS}^\dagger)$ is a *diagonal* matrix with elements $\{|\tilde{s}(c_i)|^2\}$, and $\mathbf{K}$ is the covariance matrix associated with the sequence of diffuse components $\tilde{\mathbf{a}}$ given in (10). Under the preceding assumptions on ψ, the corresponding ML decoding metric is then given by

$$m_{ML}(\tilde{\mathbf{r}}^N; \mathbf{c}^N) = - < (\tilde{\mathbf{r}}^N - \Gamma\mathbf{Su}), (\mathbf{SHS}^\dagger)^{-1}(\tilde{\mathbf{r}}^N - \Gamma\mathbf{Su}) > - \ln|\mathbf{H}| - \ln|\mathbf{B}|. \tag{28}$$

For constant-envelope modulation, $\mathbf{B}$ is the identity matrix $\mathbf{I}$, and then the ML metric corresponding to (28) simplifies to

$$m_{ML}(\tilde{\mathbf{r}}^N; \mathbf{c}^N) = 2\Gamma Re\left\{< \tilde{\mathbf{r}}^N, (\mathbf{SHS}^\dagger)^{-1}\mathbf{Su} >\right\} - < \tilde{\mathbf{r}}^N, (\mathbf{SHS}^\dagger)^{-1}\tilde{\mathbf{r}}^N > . \tag{29}$$

Furthermore, for the Rayleigh channel ($\Gamma = 0$) the first term on the right-hand side in (29) vanishes. For the case of *ideal* interleaving/deinterleaving, the corresponding ML decoding metric can be obtained from (28) simply by taking $\mathbf{K} = 2\sigma_a^2\mathbf{I}$ (i.e., the diffuse components are now assumed i.i.d.) and the corresponding ML metric can again be expressed as the sum of individual branch metrics such that

$$m_{ML}(\tilde{\mathbf{r}}^N; \mathbf{c}^N) = \sum_{i=1}^{N} m_{ML}(\tilde{r}_i; c_i), \tag{30}$$

where now

$$m_{ML}(\tilde{r}_i; c_i) = \frac{-|\tilde{r}_i|^2 + 2\Gamma Re\{\tilde{r}_i\tilde{s}^*(c_i)\} - \Gamma^2|\tilde{s}(c_i)|^2}{2\sigma_a^2|\tilde{s}(c_i)|^2 + N_0/E_s} - \ln(2\sigma_a^2|\tilde{s}(c_i)|^2 + N_0/E_s). \tag{31}$$

In particular, for constant-envelope modulation, the branch metric in (31) is equivalent to the linear metric

$$m_{ML}(\tilde{r}_i; c_i) = Re\{\tilde{r}_i \tilde{s}^*(c_i)\}. \tag{32}$$

Next, we consider the MPSK system except that we assume the input sequence has been differentially encoded prior to application to the modulator. More specifically, the components of the transmitted sequence $\mathbf{c}$ are obtained from the input sequence $\mathbf{c}'$ as $c_i = modulo(\sum_{j=0}^{i} c'_j, M)$, $i = 0, 1, \cdots$, where we assume c'_0, and hence c_0, is fixed and known to the receiver. The normalized signal components in (14) can then be written as

$$\begin{aligned} \tilde{s}(c_i) &= \prod_{j=0}^{i} \tilde{s}(c'_j) \\ &= \tilde{s}(c_0) \prod_{j=1}^{i} \tilde{s}(c'_j); \; i = 0, 1, \cdots. \end{aligned} \tag{33}$$

As in (25), the matched filter output sequence $\tilde{\mathbf{r}}^{N+1} = (\tilde{r}_0, \tilde{r}_1, \cdots, \tilde{r}_N)$ can be expressed as

$$\tilde{\mathbf{r}}^{N+1} = \tilde{s}(c_0)\mathbf{S}'\tilde{\mathbf{z}}^{N+1} + \tilde{\mathbf{n}}^{N+1}, \tag{34}$$

where we assume an initial observation $\tilde{r}_0$ which, of course, carries no information. The matrix[3] $\mathbf{S}'$ is again diagonal with corresponding elements $\{\prod_{j=1}^{i} \tilde{s}(c'_j)\}$ where we assume the leading ($i = 0$) term is unity.

It follows from (29) and the sequel that the corresponding ML metric for choosing the sequence $\mathbf{c}'^{N+1}$ with *known* initial component $c'_0 = c_0$ on the basis of the observation vector $\tilde{\mathbf{r}}^{N+1}$ is then

$$m_{ML}(\tilde{\mathbf{r}}^{N+1}; \mathbf{c}'^{N+1}) = 2\Gamma Re\left\{\tilde{s}^*(c_0) < \tilde{\mathbf{r}}^{N+1}, (\mathbf{S}'\mathbf{H}\mathbf{S}'^{\dagger})^{-1}\mathbf{S}'\mathbf{u} >\right\} - < \tilde{\mathbf{r}}^{N+1}, (\mathbf{S}'\mathbf{H}\mathbf{S}'^{\dagger})^{-1}\tilde{\mathbf{r}}^{N+1} > . \tag{35}$$

This ML metric was previously developed by Ho and Fung in [19] for the special case of the Rayleigh ($\Gamma = 0$) channel in which case the metric is purely quadratic in $\tilde{\mathbf{r}}^{N+1}$ and is independent of the initial component c_0. In the more general case considered here, this ML metric is difficult to handle analytically, including the fact that it depends explicitly upon c_0. Nevertheless, under some reasonable simplifying assumptions, we demonstrate in the next

[3]We use the prime here to emphasize the explicit dependence of $\mathbf{S}'$ on the input sequence $\mathbf{c}'^{N+1}$.

subsection that the ML metric can be approximated by the simpler and familiar MDPSK decoding metric.

III.3. M-ary Differential PSK with No CSI

Fortunately, for constant-envelope modulation, if both differential encoding and decoding are employed the ML metric for *no* CSI can again be expressed as the sum of linear branch metrics whether or not *ideal* interleaving/deinterleaving is used as we now demonstrate. First, observe that, under the first-order Gauss-Markov process assumption, the slow-fading Rician channel has a relationship between the two fading components $\tilde{z}_i$ and $\tilde{z}_{i-1}$ given by

$$\tilde{z}_i = \rho\tilde{z}_{i-1} + (1-\rho)\Gamma e^{j\psi} + \sqrt{1-\rho^2}\tilde{w}_i. \tag{36}$$

Since we assume that $\tilde{\mathbf{z}}^{N+1}$ is a first-order Gauss-Markov process, the received sequence $\tilde{\mathbf{r}}^{N+1}$ is also a first-order Gauss-Markov process given the transmitted sequence $\mathbf{c}^{N+1}$, where $\mathbf{c}^{N+1}$ is the output of a differential encoder with input sequence $\mathbf{c}'^{N+1}$. The conditional pdf $p(\tilde{\mathbf{r}}^{N+1}|\mathbf{c}^{N+1})$ is then

$$p(\tilde{\mathbf{r}}^{N+1}|\mathbf{c}^{N+1}) = p(\tilde{r}_N|\tilde{r}_{N-1},\mathbf{c}^{N+1})p(\tilde{r}_{N-1}|\tilde{r}_{N-2},\mathbf{c}^{N+1})\cdots p(\tilde{r}_2|\tilde{r}_1,\mathbf{c}^{N+1})p(\tilde{r}_1|\tilde{r}_0,\mathbf{c}^{N+1}), \tag{37}$$

where

$$\begin{aligned} p(\tilde{r}_i|\tilde{r}_{i-1},\mathbf{c}^{N+1}) &= \int_{-\infty}^{\infty} p(\tilde{r}_i|\tilde{z}_{i-1},c_i)p(\tilde{z}_{i-1}|\tilde{r}_{i-1},c_{i-1})d\tilde{z}_{i-1} \\ &= p(\tilde{r}_i|\tilde{r}_{i-1},c_i,c_{i-1}). \end{aligned} \tag{38}$$

Here, we assume that $\tilde{r}_0$ is given, possibly from the previous received sequence. Then, the corresponding ML metric is given by

$$m_{ML}(\tilde{\mathbf{r}}^{N+1};\mathbf{c}^{N+1}) = \sum_{i=1}^{N} m_{ML}(\tilde{r}_i;\tilde{r}_{i-1},c_i,c_{i-1}), \tag{39}$$

with branch metric

$$m_{ML}(\tilde{r}_i;\tilde{r}_{i-1},c_i,c_{i-1}) = \log p(\tilde{r}_i|\tilde{r}_{i-1},c_i,c_{i-1}). \tag{40}$$

Evaluation of this requires explicit evaluation of (38); we first discuss the pdf's $p(\tilde{r}_i|\tilde{z}_{i-1},c_i)$ and $p(\tilde{z}_{i-1}|\tilde{r}_{i-1},c_{i-1})$ appearing in the integrand. For simplicity, we only consider constant-envelope modulation; $|\tilde{s}(c_i)|^2$ is then unity for all i. Using the relation between $\tilde{z}_i$ and $\tilde{z}_{i-1}$

in (36), the complex demodulator output in (18) can then be rewritten as

$$\begin{aligned}\tilde{r}_i = \rho\tilde{z}_{i-1}\tilde{s}(c_i) &+ (1-\rho)\Gamma e^{j\psi}\tilde{s}(c_i) \\ &+ \tilde{s}(c_i)\sqrt{1-\rho^2}\tilde{w}_i + \frac{1}{\sqrt{E_s}}\tilde{n}_i,\end{aligned} \tag{41}$$

and the probability density function of $\tilde{r}_i$ given $(\tilde{z}_{i-1}, c_i)$ is then

$$p(\tilde{r}_i|\tilde{z}_{i-1}, c_i) = \frac{1}{2\pi\sigma^2_{r_i|z_{i-1}}}\exp\{-\frac{|\tilde{r}_i - m_{r_i|z_{i-1}}|^2}{2\sigma^2_{r_i|z_{i-1}}}\}, \tag{42a}$$

where

$$m_{r_i|z_{i-1}} = (1-\rho)\Gamma e^{j\psi}\tilde{s}(c_i) + \rho\tilde{z}_{i-1}\tilde{s}(c_i), \tag{42b}$$

and

$$2\sigma^2_{r_i|z_{i-1}} = (1-\rho^2)2\sigma_a^2 + \frac{N_0}{E_s}. \tag{42c}$$

Likewise, the probability density function of $\tilde{z}_{i-1}$ given $(\tilde{r}_{i-1}, c_{i-1})$ is given by

$$p(\tilde{z}_{i-1}|\tilde{r}_{i-1}, c_{i-1}) = \frac{1}{\pi N_0/E_s}\exp\Big\{\frac{-|\tilde{z}_{i-1} - \tilde{r}_{i-1}\tilde{s}^*(c_{i-1})|^2}{N_0/E_s}\Big\}. \tag{43}$$

After some algebraic manipulation, the integral in (38) can be expressed as

$$\begin{aligned}p(\tilde{r}_i|\tilde{r}_{i-1}, c_i, c_{i-1}) = \frac{1}{\pi\sigma^2_{\tilde{r}_i|\tilde{r}_{i-1}}}\exp\Big\{\frac{1}{\sigma^2_{\tilde{r}_i|\tilde{r}_{i-1}}}\Big[-|\tilde{r}_i|^2 - \rho^2|\tilde{r}_{i-1}|^2 - (1-\rho)^2\Gamma^2 \\ +2Re\Big\{\rho\tilde{r}_i\tilde{r}^*_{i-1}\tilde{s}^*(c_i)\tilde{s}(c_{i-1}) - (1-\rho)\Gamma e^{j\psi}[\rho\tilde{r}_{i-1}\tilde{s}^*(c_{i-1}) - \tilde{r}_i\tilde{s}^*(c_i)]\Big\}\Big]\Big\},\end{aligned} \tag{44}$$

where

$$\sigma^2_{\tilde{r}_i|\tilde{r}_{i-1}} = (1-\rho^2)2\sigma_a^2 + (\rho^2+1)N_0/E_s. \tag{45}$$

The ML branch metric can then be simplified to

$$\begin{aligned}m_{ML}(\tilde{r}_i; \tilde{r}_{i-1}, c_i, c_{i-1}) &= Re\{\rho\tilde{r}_i\tilde{r}^*_{i-1}\tilde{s}^*(c_i)\tilde{s}(c_{i-1})\} \\ &\quad +(1-\rho)\Gamma Re\Big\{e^{j\psi}[\tilde{r}^*_i\tilde{s}(c_i) - \rho\tilde{r}^*_{i-1}\tilde{s}(c_{i-1})]\Big\}.\end{aligned} \tag{46}$$

Observe that the second term in (46) is zero for the AWGN channel($\rho = 1$) as well as for the Rayleigh channel($\Gamma = 0$). Furthermore, we can also effectively ignore the second term of (46) under the slow-fading assumption since then $\rho \approx 1$. Then an approximate ML branch metric is of the form

$$m_{ML}(\tilde{r}_i; \tilde{r}_{i-1}, c_i, c_{i-1}) \approx Re\{\tilde{r}_i\tilde{r}^*_{i-1}\tilde{s}^*(c_i)\tilde{s}(c_{i-1})\}, \tag{47}$$

suggesting use of linear filtering in conjunction with differential detection. Indeed, a differential encoder should likewise be employed in this case and then, for MPSK modulation schemes, the input of the differential encoder, $\{c_i'\}$, can be expressed as

$$e^{j2\pi c_i'/M} = e^{j2\pi c_i/M} e^{-j2\pi c_{i-1}/M}, \tag{48}$$

where, as previously, the transmitted sequence $\{c_i\}$ is the output of the differential encoder. Then, the approximate ML decoding metric for the resulting M-ary differential PSK (MDPSK) scheme, is given by

$$\begin{aligned} m_{ML}(\tilde{r}_i; \tilde{r}_{i-1}, c_i') &= Re\{\tilde{r}_i \tilde{r}_{i-1}^* e^{-j2\pi c_i/M} e^{j2\pi c_{i-1}/M}\}, \\ &= Re\{\tilde{r}_i \tilde{r}_{i-1}^* e^{-j2\pi c_i'/M}\}. \end{aligned} \tag{49}$$

IV. Cutoff Rate Computations:

In this section we provide explicit evaluation of the cutoff rate R_0 for the slow-fading Rician channel model under a variety of assumptions on signaling strategies and receiver implementations. We generally evaluate the cutoff rate R_0 using a straightforward Chernoff upper bounding approach to bound the pairwise codeword error probability in the form [8]

$$Pr\{\mathbf{c} \to \hat{\mathbf{c}} \mid \mathbf{c}\} \leq \min_{\lambda \geq 0} f(\lambda; \mathbf{c}, \hat{\mathbf{c}}), \tag{50}$$

where for the case of *perfect* CSI

$$f(\lambda; \mathbf{c}, \hat{\mathbf{c}}) \triangleq E\Big\{E\{e^{\lambda[m_{ML}(\tilde{\mathbf{r}}; \hat{\mathbf{c}}, \tilde{\mathbf{z}}) - m_{ML}(\tilde{\mathbf{r}}; \mathbf{c}, \tilde{\mathbf{z}})]} \mid \mathbf{c}, \tilde{\mathbf{z}}\}\Big\}, \tag{51}$$

while for the case of *no* CSI

$$f(\lambda; \mathbf{c}, \hat{\mathbf{c}}) \triangleq E\{e^{\lambda[m_{ML}(\tilde{\mathbf{r}}; \hat{\mathbf{c}}) - m_{ML}(\tilde{\mathbf{r}}; \mathbf{c})]} \mid \mathbf{c}\}. \tag{52}$$

Now the average error probability in choosing between two randomly selected codewords of length N' can be bounded as

$$\overline{P_{e,N'}} \leq \min_{\lambda \geq 0} \sum_{\mathbf{c}^{N'}, \hat{\mathbf{c}}^{N'}} Q(\mathbf{c}^{N'}) Q(\hat{\mathbf{c}}^{N'}) f(\lambda; \mathbf{c}^{N'}, \hat{\mathbf{c}}^{N'}), \tag{53}$$

where any codeword $\mathbf{c}^{N'}$ is chosen independently with product measure

$$Q(\mathbf{c}^{N'}) = \prod_{i=1}^{N'} Q(c_i). \tag{54}$$

Then the cutoff rate R_0, in bits/channel use, is defined as

$$R_0 = \lim_{N' \to \infty} \max_{\mathbf{Q}} \max_{\lambda \geq 0} R_{0,N'}(\mathbf{Q}, \lambda), \tag{55}$$

where

$$R_{0,N'}(\mathbf{Q}, \lambda) = -\frac{1}{N'} \log_2 \sum_{\mathbf{c}^{N'}, \hat{\mathbf{c}}^{N'}} Q(\mathbf{c}^{N'}) Q(\hat{\mathbf{c}}^{N'}) f(\lambda; \mathbf{c}^{N'}, \hat{\mathbf{c}}^{N'}), \tag{56}$$

with $\mathbf{Q} = (Q(0), Q(1), Q(2), ..., Q(M-1))$ representing the marginal distribution on the input channel signaling alphabet.

Consider *ideal* interleaving/deinterleaving of subsequences of fixed length[4] N resulting in the sequence $\{\mathbf{c}_l^N\}$. More specifically, we assume $N' = LN$ such that $\mathbf{c}^{N'} = (\mathbf{c}_1^N, \mathbf{c}_2^N, \cdots, \mathbf{c}_L^N)$ with $\mathbf{c}_l^N = (c_{(l-1)N+1}, c_{(l-1)N+2}, \cdots, c_{(l-1)N+N})$. Then we have

$$f(\lambda; \mathbf{c}^{N'}, \hat{\mathbf{c}}^{N'}) = \prod_{l=1}^{L} f(\lambda; \mathbf{c}_l^N, \hat{\mathbf{c}}_l^N). \tag{57}$$

In follows, in particular, that then

$$\begin{aligned} R_{0,N'}(\mathbf{Q}, \lambda) &= -\frac{1}{LN} \log_2 \sum_{\mathbf{c}_1^N, \hat{\mathbf{c}}_1^N} \cdots \sum_{\mathbf{c}_L^N, \hat{\mathbf{c}}_L^N} \prod_{l=1}^{L} Q(\mathbf{c}_l^N) Q(\hat{\mathbf{c}}_l^N) f(\lambda; \mathbf{c}_l^N, \hat{\mathbf{c}}_l^N) \\ &= -\frac{1}{N} \log_2 \sum_{\mathbf{c}_l^N, \hat{\mathbf{c}}_l^N} Q(\mathbf{c}_l^N) Q(\hat{\mathbf{c}}_l^N) f(\lambda; \mathbf{c}_l^N, \hat{\mathbf{c}}_l^N). \\ &= R_{0,N}(\mathbf{Q}, \lambda), \end{aligned} \tag{58}$$

so that from (55)

$$R_0 = \max_{\mathbf{Q}} \max_{\lambda \geq 0} R_{0,N}(\mathbf{Q}, \lambda), \tag{59}$$

and R_0 is determined by the N-tuple transmission characteristics of the channel.

Furthermore, as shown in Appendix 5C [8], the optimizing input distribution $\mathbf{Q}^*$ for a *symmetric* channel is equiprobable (i.e., $Q^*(m) = 1/M, m = 0, 1, ..., M-1$). More specifically, the input distribution $Q(c_i)$ is equiprobable if

$$\sum_{\mathbf{c}^N} f(\lambda^*; \mathbf{c}^N, \hat{\mathbf{c}}^N) = \text{constant for all } \hat{\mathbf{c}}^N. \tag{60}$$

[4]Note that conventional symbol-by-symbol interleaving/deinterleaving corresponds to the case $N = 1$. We consider the more general case here to allow investigation of channel memory effects.

This holds, in particular, for MPSK. On the other hand, for QAM schemes the optimizing input distribution is not equiprobable as shown, for example, in [8] for PAM. To simplify matters we will also use the equiprobable input distribution for QAM although this is clearly suboptimum in this case. Nevertheless, with this choice the cutoff rate $R_{0,N} = R_{0,N}(\mathbf{Q}^*, \lambda^*)$ for *ideal* interleaving/deinterleaving of subsequences of length N is then given by

$$R_{0,N} = -\frac{1}{N}\log_2 \frac{1}{M^{2N}} \sum_{\mathbf{c}^N, \hat{\mathbf{c}}^N} f(\lambda^*; \mathbf{c}^N, \hat{\mathbf{c}}^N), \tag{61}$$

where λ^* is the optimized value of λ. For the case of MPSK, the condition in (60) holds, and the cutoff rate in (61) then simplifies to

$$R_{0,N} = -\frac{1}{N}\log_2 \frac{1}{M^{N}} \sum_{\mathbf{c}^N} f(\lambda^*; \mathbf{c}^N, \hat{\mathbf{c}}^N), \tag{62}$$

which is constant for all $\hat{\mathbf{c}}^N$. For simplicity, we choose $\hat{\mathbf{c}}^N = (0, 0, \cdots, 0)$ for evaluation of $R_{0,N}$ for MPSK.

For the case of differential encoding of MPSK this development must be modified somewhat to account for the need to periodically transmit a known reference symbol at the beginning of each subsequence of length N. The corresponding cutoff rate $R'_{0,N}$ is then given by[5]

$$R'_{0,N} = -\frac{1}{N}\log_2 \frac{1}{M^{2N}} \sum_{\mathbf{c}'^{N+1}, \hat{\mathbf{c}}'^{N+1}} f(\lambda^*; \mathbf{c}'^{N+1}, \hat{\mathbf{c}}'^{N+1}), \tag{63}$$

where the summation is over all M^{2N} pairs of sequences $\mathbf{c}'^{N+1}, \hat{\mathbf{c}}'^{N+1}$ of length $N+1$ with c_0 in the initial position. Again, in this case, the condition in (60) holds, and the cutoff rate in (63) can be simplified to

$$R'_{0,N} = -\frac{1}{N}\log_2 \frac{1}{M^{N}} \sum_{\mathbf{c}'^{N+1}} f(\lambda^*; \mathbf{c}'^{N+1}, \mathbf{0}^{N+1}), \tag{64}$$

where $\mathbf{0}^{N+1} = (0, 0, \cdots, 0)$, the all-zero sequence of length $N+1$.

IV.1. Memoryless Modulation with Perfect CSI

As discussed previously, for the case of *perfect* CSI, the ML decoding metric is simply the sum of the individual *branch metrics* whether or not interleaving/deinterleaving is used

[5]In the particular case of the Rayleigh channel, the factor $1/(N+1)$ here is replaced by $1/N$ to reflect the previously noted fact that the known reference symbol c_0 is not required in this case.

and thus from (51) we have

$$f(\lambda; \mathbf{c}^N, \hat{\mathbf{c}}^N) = E\Big\{\prod_{i=1}^{N} f_p(\lambda; c_i, \hat{c}_i, \tilde{z}_i)\Big\}, \tag{65a}$$

where

$$f_p(\lambda; c_i, \hat{c}_i, \tilde{z}_i) \triangleq E\Big\{e^{\lambda[m_{ML}(\tilde{r}_i;\hat{c}_i,\tilde{z}_i) - m_{ML}(\tilde{r}_i;c_i,\tilde{z}_i)]} \mid c_i, \tilde{z}_i\Big\}, \tag{65b}$$

and for the *perfect* CSI case the optimizing value of λ is easily shown to be $\lambda^* = 1/2$. Furthermore, after some simple algebra, in this case we have

$$f_p(\lambda^*; c_i, \hat{c}_i, \tilde{z}_i) = \exp\left\{-\frac{E_s}{4N_0}|\tilde{z}_i|^2 d_E^2(c_i, \hat{c}_i)\right\}, \tag{66a}$$

where $d_E^2(c_i, \hat{c}_i)$ is the squared Euclidean distance

$$d_E^2(c_i, \hat{c}_i) \triangleq |\tilde{s}(c_i) - \tilde{s}(\hat{c}_i)|^2. \tag{66b}$$

Substituting (66) into (61), we have

$$R_{0,N} = -\frac{1}{N}\log_2 \frac{1}{M^{2N}} \sum_{c_1,\hat{c}_1} \cdots \sum_{c_N,\hat{c}_N} E\Big\{\exp\{-\frac{E_s}{4N_0} < \tilde{\mathbf{z}}^N, \mathbf{D}\tilde{\mathbf{z}}^N >\}\Big\}, \tag{67}$$

where $\mathbf{D}$ is the *diagonal* matrix in the elements $\{d_E^2(c_i, \hat{c}_i)\}$ defined in (66b). We assume that $\tilde{\mathbf{z}}^N$ is the first-order Gauss-Markov process with pdf $p(\tilde{\mathbf{z}}^N)$ given by (9), and then (67) can be written as

$$\begin{aligned} R_{0,N} &= 2\log_2 M - \frac{1}{N}\log_2\Big(\sum_{c_1,\hat{c}_1} \cdots \sum_{c_N,\hat{c}_N} \int \exp\{-\frac{E_s}{4N_0} < \tilde{\mathbf{z}}^N, \mathbf{D}\tilde{\mathbf{z}}^N >\} p(\tilde{\mathbf{z}}^N) d\tilde{\mathbf{z}}^N\Big) \\ &= 2\log_2 M - \frac{1}{N}\log_2\Big(\sum_{c_1,\hat{c}_1} \cdots \sum_{c_N,\hat{c}_N} |\mathbf{H_d}| \exp\{\Gamma^2 < \mathbf{u}, (\mathbf{H_d}\mathbf{K}^{-1} - \mathbf{K}^{-1})\mathbf{u} >\}\Big), \end{aligned} \tag{68a}$$

where

$$\mathbf{H_d} = \Big(\mathbf{I} + \frac{E_s}{4N_0}\mathbf{K}\mathbf{D}\Big)^{-1}. \tag{68b}$$

For the Rayleigh channel ($\Gamma = 0$), this simplifies to

$$R_{0,N} = 2\log_2 M - \frac{1}{N}\log_2\Big(\sum_{c_1,\hat{c}_1} \cdots \sum_{c_N,\hat{c}_N} |\mathbf{H_d}|\Big). \tag{69}$$

The results in (68) and (69) were also evaluated in [18] although in somewhat less generality.

Considering the case of $\rho = 1$, $\tilde{z}_n$ is constant for all n. Direct substitution of this constant value $\tilde{z}_n$ into (61) yields

$$R_{0,N} = -\frac{1}{N}\log_2\Big(\sum_{c_1,\hat{c}_1}\cdots\sum_{c_N,\hat{c}_N}\frac{1}{M^{2N}}E\Big\{\exp\{-\frac{E_s}{4N_0}|\tilde{z}_n|^2\sum_{i=1}^{N}d_E^2(c_i,\hat{c}_i)\}\Big\}\Big), \tag{70}$$

and, after some algebra, it can be shown that

$$\begin{aligned} E\Big\{\exp\{-\frac{E_s}{4N_0}|\tilde{z}_n|^2\sum_{i=1}^{N}d_E^2(c_i,\hat{c}_i)\}\Big\} &= \frac{1+\zeta^2}{1+\zeta^2+\frac{E_s}{4N_0}\sum_{i=1}^{N}d_E^2(c_i,\hat{c}_i)} \\ &\quad\cdot\exp\Big\{-\frac{E_s}{4N_0}\frac{\zeta^2\sum_{i=1}^{N}d_E^2(c_i,\hat{c}_i)}{1+\zeta^2+\frac{E_s}{4N_0}\sum_{i=1}^{N}d_E^2(c_i,\hat{c}_i)}\Big\}, \end{aligned} \tag{71}$$

where, as previously described, the quantity $\zeta^2 = \Gamma^2/2\sigma_a^2$ represents the ratio of specular-to-diffuse energy. For the Rayleigh channel ($\zeta^2 = 0$) this reduces to

$$\begin{aligned} R_{0,N} &= -\frac{1}{N}\log_2\Big(\sum_{c_1,\hat{c}_1}\cdots\sum_{c_N,\hat{c}_N}\frac{1}{M^{2N}}\frac{1}{1+\frac{E_s}{4N_0}\sum_{i=1}^{N}d_E^2(c_i,\hat{c}_i)}\Big) \\ &= -\frac{1}{N}\log_2\Big(\sum_{c_1,\hat{c}_1}\cdots\sum_{c_N,\hat{c}_N}\frac{1}{M^{2N}}\int_0^1 u^{\frac{E_s}{4N_0}\sum_{i=1}^{N}d_E^2(c_i,\hat{c}_i)}du\Big) \\ &= -\frac{1}{N}\log_2\int_0^1\Big(\frac{1}{M^2}\sum_{c_i,\hat{c}_i}u^{\frac{E_s}{4N_0}d_E^2(c_i,\hat{c}_i)}\Big)^N du. \end{aligned} \tag{72}$$

As shown in Appendix B, for finite E_s/N_0, in this special case we have

$$\lim_{N\to\infty} R_{0,N} = 0. \tag{73}$$

Therefore, without interleaving/deinterleaving, memoryless modulation schemes are useless when $\rho = 1$.

For the case of *ideal* interleaving/deinterleaving on an individual symbol basis ($N = 1$), we can evaluate the cutoff rate $R_{0,1}$ from (68) under the substitution $\mathbf{K} = \frac{1}{2\sigma_a^2}$ with the result

$$R_{0,1} = 2\log_2 M - \log_2\Big(\sum_{c_1,\hat{c}_1}\exp\{-\frac{E_s}{4N_0}d_{ME}^2(c_i,\hat{c}_i)\}\Big), \tag{74}$$

where $d_{ME}^2(c_i,\hat{c}_i)$ is the *modified* Euclidean distance

$$d_{ME}^2(c_i,\hat{c}_i) = \frac{\zeta^2 d_E^2(c_i,\hat{c}_i)}{1+\zeta^2+\frac{E_s}{4N_0}d_E^2(c_i,\hat{c}_i)} + \Big(\frac{E_s}{4N_0}\Big)^{-1}\ln\frac{1+\zeta^2+\frac{E_s}{4N_0}d_E^2(c_i,\hat{c}_i)}{1+\zeta^2}. \tag{75}$$

The result in (74) was also obtained by Divsalar and Simon [14].

IV.2. Memoryless Modulation with No CSI

As shown in Section III.2, the ML decoding rule, especially for QAM, is quite complicated when CSI is not available. As a result, we consider only the case of constant-envelope modulation, so that from (26) the corresponding pdf $p(\tilde{\mathbf{r}}^N|\mathbf{c}^N)$ is given by

$$p(\tilde{\mathbf{r}}^N|\mathbf{c}^N) = \frac{1}{\pi^N|\mathbf{H}|}\exp\left\{- < (\tilde{\mathbf{r}}^N - \Gamma\mathbf{Su}), (\mathbf{SHS}^\dagger)^{-1}(\tilde{\mathbf{r}}^N - \Gamma\mathbf{Su}) >\right\}, \tag{76}$$

where

$$\mathbf{H} = \mathbf{K} + (N_0/E_s)\mathbf{I}. \tag{77}$$

Then we evaluate the expectation in (52) using (29) and (76) with the result

$$\begin{aligned} f(\lambda; \mathbf{c}^N, \hat{\mathbf{c}}^N) &= \int_{-\infty}^{\infty} e^{\lambda[m_{ML}(\tilde{\mathbf{r}}^N;\hat{\mathbf{c}}^N) - m_{ML}(\tilde{\mathbf{r}}^N;\mathbf{c}^N)]} p(\tilde{\mathbf{r}}^N|\mathbf{c}^N) d\mathbf{r}^N \\ &= \frac{|\mathbf{F}(\lambda)|}{|\mathbf{H}|}\exp\Big\{\Gamma^2 < (\mathbf{I} + \lambda\hat{\mathbf{B}} - \lambda\mathbf{I})\mathbf{H}^{-1}\mathbf{u}, \mathbf{F}(\lambda)(\mathbf{I} + \lambda\hat{\mathbf{B}} - \lambda\mathbf{I})\mathbf{H}^{-1}\mathbf{u} > \\ &\qquad -\Gamma^2 < \mathbf{u}, \mathbf{H}^{-1}\mathbf{u} >\Big\}, \end{aligned} \tag{78}$$

where

$$\mathbf{F}(\lambda) = \left(\mathbf{H}^{-1} + \lambda\hat{\mathbf{B}}\mathbf{H}^{-1}\hat{\mathbf{B}}^\dagger - \lambda\mathbf{H}^{-1}\right)^{-1}, \tag{79}$$

with $\hat{\mathbf{B}}$ the $N \times N$ *diagonal* matrix in the elements $\{e^{j2\pi(\hat{c}_i - c_i)/M}\}$. Substituting (78) into (61), we can evaluate the cutoff rate $R_{0,N}$ with λ^*, the optimized value of λ. For the Rayleigh channel, $\lambda^* = 1/2$ and the cutoff rate $R_{0,N}$ then simplifies to

$$R_{0,N} = -\frac{1}{N}\log_2 \frac{1}{M^{2N}} \sum_{\mathbf{c}^N, \hat{\mathbf{c}}^N} \frac{|\mathbf{F}(1/2)|}{|\mathbf{H}|}. \tag{80}$$

Now, consider the cutoff rate $R_{0,1}$ for MPSK with *no* CSI for the case of *ideal* interleaving/deinterleaving on a symbol basis ($N = 1$). In this case, the common covariance matrix $\mathbf{H}$ in (78) simplifies to the scalar value

$$\mathbf{H} = 1/(2\sigma_a^2 + N_0/E_s), \tag{81}$$

and $\hat{\mathbf{B}}\mathbf{H}\hat{\mathbf{B}}^\dagger$ is simply equal to $\mathbf{H}$ and the terms in λ in (79) cancel. It follows that then $\mathbf{F}(\lambda) = \mathbf{H}$. Substituting these values of $\mathbf{H}$ and $\mathbf{F}(\lambda)$ in (81) into (78), the cutoff rate can be expressed as

$$R_{0,1} = -\log_2 \sum_{c_i, \hat{c}_i} \frac{1}{M^2}\exp\{-\frac{E_s}{4N_0} d'^2_{ME}(c_i, \hat{c}_i)\}, \tag{82}$$

where we define a new *modified* Euclidean distance

$$d'^2_{ME}(c_i,\hat{c}_i) \triangleq \frac{\zeta^2 d_E^2(c_i,\hat{c}_i)}{1+\zeta^2+\frac{E_s}{N_0}}. \tag{83}$$

For $\zeta = \infty$, the *modified* Euclidean distance in (83) is equal, as expected, to the ordinary Euclidean distance appropriate for the AWGN channel.

We now consider the cutoff rate performance of MPSK schemes for the case of *ideal* interleaving/deinterleaving of symbols ($N = 1$) with infinite E_s/N_0 and define

$$R_{0,\max}(\zeta^2) \triangleq \lim_{E_s/N_0\to\infty} R_{0,1} \ ; \ \text{bits/c.u.}, \tag{84}$$

where $R_{0,1}$ is given in (82) for the *no* CSI case. It follows then that

$$R_{0,\max}(\zeta^2) = -\log_2 \sum_{c_i,\hat{c}_i} \frac{1}{M^2} \exp\left\{-\frac{\zeta^2}{4} d_E^2(c_i,\hat{c}_i)\right\}. \tag{85}$$

Proceeding as in (62) and the sequel, this simplifies to

$$R_{0,\max}(\zeta^2) = \log_2 M - \log_2 \sum_{c_i=0}^{M-1} \exp\left\{-\frac{\zeta^2}{4} d_E^2(c_i,0)\right\}. \tag{86}$$

The quantity $R_{0,\max}$ is *independent* of E_b/N_0 and depends only upon ζ^2, which represents a measure of the *useful* signal component in this case. Note that for the Rayleigh channel (ζ^2=0) we have $R_{0,\max}(0) = 0$, in which case MPSK is useless when CSI is not available, as was to be expected.

In Fig. 2, we illustrate the asymptotic cutoff rate, $R_{0,\max}$, for MPSK as $E_s/N_0 \to \infty$. Observe that the maximum signaling rate cannot be increased by increasing M except for very large ζ^2. For example, with $\zeta^2 = 10$dB the maximum signaling rate is limited to approximately 2.5 bits/channel use *regardless* of the value of M. This would indicate that, in the absence of CSI, it is impossible to achieve high signaling rates with *ideal* interleaving/deinterleaving of symbols ($N = 1$) for severe fading; $\zeta^2 \leq 10$dB say.

Next, we consider the MPSK system employing differential encoding and making use of a previous symbol $\tilde{r}_0$ when a transmitted reference symbol c_0 is available. Proceeding as in (35) and the sequel, we have

$$\begin{aligned} f(\lambda;\mathbf{c}'^{N+1},\hat{\mathbf{c}}'^{N+1}) &= \int_{-\infty}^{\infty} e^{\lambda[m_{ML}(\tilde{\mathbf{r}}^{N+1};\hat{\mathbf{c}}'^{N+1})-m_{ML}(\tilde{\mathbf{r}}^{N+1};\mathbf{c}'^{N+1})]} p(\tilde{\mathbf{r}}^{N+1}|\mathbf{c}'^{N+1}) d\tilde{\mathbf{r}}^{N+1} \\ &= \frac{|\mathbf{F}(\lambda)|}{|\mathbf{H}|} \exp\Big\{\Gamma^2 < (\mathbf{I}+\lambda\hat{\mathbf{B}}-\lambda\mathbf{I})\mathbf{H}^{-1}\mathbf{u}, \\ &\qquad \mathbf{F}(\lambda)(\mathbf{I}+\lambda\hat{\mathbf{B}}-\lambda\mathbf{I})\mathbf{H}^{-1}\mathbf{u} > -\Gamma^2 < \mathbf{u},\mathbf{H}^{-1}\mathbf{u} >\Big\}, \end{aligned} \tag{87}$$

where $\mathbf{F}(\lambda)$ and $\mathbf{H}$ are the corresponding $(N+1)\times(N+1)$ matrices associated with $\tilde{\mathbf{r}}^{N+1}$. The corresponding cutoff rate $R'_{0,N}$ determined according to (63) is difficult to evaluate for arbitrary Γ. However, for the Rayleigh channel $R'_{0,N}$ is readily evaluated. In particular, we then have, corresponding to the previous result in (80), the expression

$$R'_{0,N} = -\frac{1}{N}\log_2 \frac{1}{M^{2N}} \sum_{\mathbf{c}'^{N+1},\hat{\mathbf{c}}'^{N+1}} \frac{|\mathbf{F}(1/2)|}{|\mathbf{H}|}, \tag{88}$$

where, as noted previously, the factor $N+1$ in (63) is replaced by $1/N$ and the summation in (88) is over all $\mathbf{c}'^{N+1}$ $\hat{\mathbf{c}}'^{N+1}$ with identical but unknown initial value c_0. Finally, after some algebraic manipulation, it can be shown that for the Rayleigh channel

$$R'_{0,N} = \frac{N+1}{N} R_{0,N+1} \tag{89}$$

where $R_{0,N+1}$ is the corresponding cutoff rate for MPSK modulation given by (80). The trick here is to recognize that the summation in (80), now over $(N+1)$-tuples $\mathbf{c}'^{N+1}$ and $\hat{\mathbf{c}}'^{N+1}$, is the same for each pair $(c_0, \hat{c}_0)$ of which there are a total of M^2 combinations. According to (89), when CSI is not available, the cutoff rate $R'_{0,N}$ for MDPSK is greater than $R_{0,N+1}$ for MPSK for $N = 1, 2, \cdots$, and $R_{0,1}$ is zero for the Rayleigh channel as shown in (82). Therefore, for the case of *no* CSI, differential encoding/decoding should be employed for the Rayleigh channel and we will discuss the corresponding cutoff rate performance for MDPSK for different values of N.

IV.3. M-ary Differential PSK with No CSI

As discussed in Section III.3, for MDPSK with *no* CSI, the ML decoding metric is simply the sum of the individual *branch metrics* whether or not interleaving/deinterleaving is used where the *branch metrics* can be approximated by the linear metric of (49). Then, corresponding to (65), we have

$$f(\lambda; \mathbf{c}'^{N}, \hat{\mathbf{c}}'^{N}) = E\Big\{\prod_{i=1}^{N} f_d(\lambda; c'_i, \hat{c}'_i, \tilde{r}_{i-1})\Big\}, \tag{90a}$$

where

$$f_d(\lambda; c'_i, \hat{c}'_i, \tilde{r}_{i-1}) \triangleq E\Big\{e^{\lambda[m_{ML}(\tilde{r}_i;\hat{c}'_i,\tilde{r}_{i-1}) - m_{ML}(\tilde{r}_i;c'_i,\tilde{r}_{i-1})]} \mid c'_i, \tilde{r}_{i-1}\Big\}, \tag{90b}$$

and c'_i is the input of the differential encoder. Here, we only consider the case of *ideal* interleaving/deinterleaving of symbols ($N = 1$), in which case

$$f(\lambda; \mathbf{c}'^N, \hat{\mathbf{c}}'^N) = \prod_{i=1}^{N} f(\lambda; c'_i, \hat{c}'_i), \tag{91}$$

where

$$f(\lambda; c'_i, \hat{c}'_i) = E\{f_d(\lambda; c'_i, \hat{c}'_i, \tilde{r}_{i-1})\}. \tag{92}$$

In Appendix A (A.22), by straightforward Chernoff bounding techniques, it is shown that for the Rician channel with large ζ^2 and E_s/N_0, and using the optimizing value of λ, this last term is approximated by

$$f(\lambda^*; c'_i, \hat{c}'_i) \approx \exp\{-\frac{E_s}{4N_0} d''^2_{ME}(c'_i, \hat{c}'_i)\}, \tag{93}$$

where now the corresponding *modified* Euclidean distance is

$$d''^2_{ME}(c'_i, \hat{c}'_i) \triangleq \frac{\frac{1}{2}\zeta^2 d^2_E(c'_i, \hat{c}'_i)}{U} + (\frac{E_s}{4N_0})^{-1} \ln \frac{U}{1 + \zeta^2 + \frac{E_s}{N_0}(1-\rho)}, \tag{94}$$

with

$$U = 1 + \zeta^2 + \frac{E_s}{N_0}(1-\rho) + (\frac{E_s}{4N_0}\rho - \frac{E_s}{16N_0}(1+\rho) - \frac{1+\zeta^2}{16}) d^2_E(c'_i, \hat{c}'_i). \tag{95}$$

Assuming $\rho = 1$, corresponding to $B_0 T_s = 0$, the expression in (94) can be simplified to

$$d''^2_{ME}(c'_i, \hat{c}'_i) = \frac{\frac{1}{2}\zeta^2 d^2_E(c'_i, \hat{c}'_i)}{1 + \zeta^2 + (\frac{E_s}{8N_0} - \frac{1+\zeta^2}{16}) d^2_E(c'_i, \hat{c}'_i)} + (\frac{E_s}{4N_0})^{-1} \ln \frac{1 + \zeta^2 + (\frac{E_s}{8N_0} - \frac{1+\zeta^2}{16}) d^2_E(c'_i, \hat{c}'_i)}{1 + \zeta^2}, \tag{96}$$

and, in particular, for the AWGN channel ($\zeta^2 = \infty$), the *modified* Euclidean distance is given by

$$d''^2_{ME}(c'_i, \hat{c}'_i) = \frac{\frac{1}{2} d^2_E(c'_i, \hat{c}'_i)}{1 - \frac{d^2_E(c'_i, \hat{c}'_i)}{16}} + (\frac{E_s}{4N_0})^{-1} \ln[1 - \frac{d^2_E(c'_i, \hat{c}'_i)}{16}]. \tag{97}$$

For the case of $\rho = 1$, the *modified* Euclidean distance in (96) was also evaluated by Divsalar and Simon in [14].

For the Rayleigh channel, as shown in (A.26), the corresponding expression for (92) is given by

$$f(\lambda^*; c'_i, \hat{c}'_i) = \frac{((1-\rho) + N_0/E_s)((1+\rho) + N_0/E_s)}{\rho^2 d^2_E(c'_i, \hat{c}'_i)/4 + ((1-\rho) + N_0/E_s)((1+\rho) + N_0/E_s)}, \tag{98}$$

or

$$f(\lambda^*; c_i', \hat{c}_i') = \frac{1}{\alpha d_E^2(c_i', \hat{c}_i')/4 + 1}, \tag{99}$$

where

$$\alpha = \rho^2/[((1-\rho) + N_0/E_s)((1+\rho) + N_0/E_s)]. \tag{100}$$

For $\rho = 1$ the quantity α reduces to

$$\alpha = \frac{E_s/N_0}{2 + N_0/E_s}. \tag{101}$$

Proceeding as in (60) and the sequel, it's easily seen that the optimizing input distribution is equiprobable, and we have

$$R_{0,1}' = \log_2 M - \log_2 \sum_{c_i'=0}^{N} \exp\{-\frac{E_s}{4N_0} d_{ME}''^2(c_i', 0)\}. \tag{102}$$

Furthermore, we now have the limiting cutoff result for the Rician channel with large ζ^2 given by[6]

$$\begin{aligned} R_{0,\max}(\zeta^2, \rho) &\triangleq \lim_{E_s/N_0 \to \infty} R_{0,1}'; \text{ bits/c.u.} \\ &= -\log_2 \frac{1}{M} \sum_{c_i'=0}^{M-1} \frac{1-\rho}{1-\rho + \frac{3\rho-1}{16} d_E^2(c_i', 0)} \exp\Big\{\frac{-\zeta^2 d_E^2(c_i', 0)/8}{1-\rho + \frac{3\rho-1}{16} d_E^2(c_i', 0)}\Big\}, \end{aligned} \tag{103}$$

and for the Rayleigh channel ($\zeta^2 = 0$) given by

$$\begin{aligned} R_{0,\max}(\rho) &\triangleq \lim_{E_s/N_0 \to \infty} R_{0,1}; \text{ bits/c.u.} \\ &= -\log_2 \frac{1}{M} \sum_{c_i'=0}^{M-1} \frac{1}{\frac{\rho^2 d_E^2(c_i', 0)}{4(1-\rho^2)} + 1}. \end{aligned} \tag{104}$$

As we can see, the quantity $R_{0,\max}$ in (103) depends upon ζ^2 and ρ, and it goes to infinity when ρ goes to unity. For the Rayleigh channel (ζ^2=0), the quantity $R_{0,\max}$ in (104) is limited by ρ as illustrated in Fig. 3. Observe that the quantity $R_{0,\max}$ is monotonically increasing for $0 \leq \rho \leq 1$. On the other hand, for MPSK schemes with *no* CSI, it follows from (86) that $R_{0,\max}(0) = 0$ for the Rayleigh channel (ζ^2=0), and the modulation scheme is useless. Therefore, for the case of *no* CSI, MDPSK schemes can be expected to have much better performance than MPSK schemes when ρ is close to unity and ζ^2 is relatively small.

[6]Unlike the case for *ideal* interleaving/deinterleaving of MPSK developed in (84) and the sequel, the limiting value of $R_{0,1}$ now depends explicitly upon ρ as well as ζ^2.

V. Limiting Cutoff Rate Performance:

Assuming *ideal* interleaving/deinterleaving of symbols ($N = 1$) is employed, the cutoff rate $R_{0,1}$, in bits/channel use, was evaluated in the previous section for *fixed* M as a function of the channel parameters. In this section, still assuming *ideal* interleaving/deinterleaving of symbols ($N = 1$), we determine the limiting cutoff rate performance when the restriction of a fixed alphabet size, M, is removed. For this case, the limiting cutoff rate $R_{0,1}$, in bits/channel use, is defined as

$$R_{0,1} = \lim_{M\to\infty} -\log_2 \sum_{c_i=0}^{M-1} \sum_{\hat{c}_i=0}^{M-1} Q^*(c_i)Q^*(\hat{c}_i) f(\lambda^*; c_i, \hat{c}_i), \tag{105}$$

where the bound function on the pairwise error probability is denoted

$$\begin{aligned} f(\lambda^*; c_i, \hat{c}_i) &= f_p(\lambda^*; c_i, \hat{c}_i); \text{ for } \textit{perfect} \text{ CSI} \\ &= f_n(\lambda^*; c_i, \hat{c}_i); \text{ for } \textit{no} \text{ CSI}, \end{aligned} \tag{106}$$

and λ^* and $Q^*(\cdot)$ are the optimizing choices for λ and $Q(\cdot)$, respectively. Here, for the case of *perfect* CSI, the bound function on the pairwise error probability is given by

$$f_p(\lambda^*; c_i, \hat{c}_i) = \exp\{-\frac{E_s}{4N_0} d^2_{ME}(c_i, \hat{c}_i)\}, \tag{107}$$

where the *modified* Euclidean distance $d^2_{ME}(c_i, \hat{c}_i)$ is described in (75). When CSI is not available, the ML decoding rule is quite complicated for QAM schemes, and we consider only the case of constant-envelope modulation. Then the bound function of the pairwise error probability is given by

$$f_n(\lambda^*; c_i, \hat{c}_i) = \exp\{-\frac{E_s}{4N_0} d'^2_{ME}(c_i, \hat{c}_i)\}, \tag{108}$$

with the *modified* Euclidean distance $d'^2_{ME}(c_i, \hat{c}_i)$ given in (83). For the case of MDPSK with *no* CSI, we use the *modified* Euclidean distance $d''^2_{ME}(c_i, \hat{c}_i)$ in (94) instead of $d'^2_{ME}(c_i, \hat{c}_i)$.

First, we consider the case of phase-only modulation. For MPSK schemes, the optimizing input distribution is equiprobable and, for the case of $M \to \infty$, we assume the optimizing input distribution on phase is uniformly distributed on $[-\pi, \pi]$. Then the limiting cutoff rate $R_{0,1}$ can be written as

$$R_{0,1} = -\log_2\left(\frac{1}{2\pi}\right)^2 \int_{-\pi}^{\pi}\int_{-\pi}^{\pi} f(\lambda^*; c_i, \hat{c}_i) d\phi(c_i) d\phi(\hat{c}_i), \tag{109}$$

where $\phi(c_i)$ is the phase of the signaling element $\tilde{s}(c_i)$. Then, as shown in [3], this simplifies to

$$R_{0,1} = -\log_2 \frac{1}{2\pi} \int_{-\pi}^{\pi} f'(\lambda^*; \psi) d\psi, \tag{110}$$

where $f'(\lambda^*; \psi)$ is equal to $f(\lambda^*; c_i, 0)$ with the substitution of the phase difference ψ between $\phi(c_i)$ and $\phi(0)$.

For the slow-fading Rician channel with *perfect* CSI, the limiting cutoff rate, as described in [3], must be evaluated by numerical intergration according to

$$R_{0,1} = -\log_2 \frac{1}{2\pi} \int_{-\pi}^{\pi} f'_p(\lambda^*; \psi) d\psi, \tag{111}$$

where

$$f'_p(\lambda^*; \psi) = \exp\{-\frac{E_s}{4N_0} d^2_{ME}(\psi)\}, \tag{112}$$

with

$$d^2_{ME}(\psi) = \frac{\zeta^2 d^2_E(\psi)}{1 + \zeta^2 + \frac{E_s}{4N_0} d^2_E(\psi)} + \left(\frac{E_s}{4N_0}\right)^{-1} \ln \frac{1 + \zeta^2 + \frac{E_s}{4N_0} d^2_E(\psi)}{1 + \zeta^2}, \tag{113}$$

and $d^2_E(\psi) = 4\sin^2(\psi/2)$. For large enough E_s/N_0 we have

$$R_{0,1} = -\log_2 \frac{e^{-\zeta^2}}{2\pi} \int_{-\pi}^{\pi} \frac{d\psi}{1 + \frac{(E_s/N_0)}{1+\zeta^2} \sin^2(\psi/2)}, \tag{114}$$

or

$$R_{0,1} = -\log_2 \frac{e^{\zeta^2}}{\sqrt{1 + \frac{E_s/N_0}{1+\zeta^2}}}. \tag{115}$$

It's of interest to observe the limiting behavior for the two extreme cases $\zeta^2 = \infty$ (the AWGN channel) and $\zeta^2 = 0$ (the Rayleigh channel). For $\zeta^2 = \infty$, we find from (113) that $d^2_{ME}(\psi) = d^2_E(\psi)$, and hence, as shown in [3], the limiting cutoff rate for the AWGN channel is given by

$$\begin{aligned} R_{0,1} &= -\log_2 \frac{1}{2\pi} \int_{-\pi}^{\pi} \exp\{-E_s/N_0 \sin^2(\psi/2)\} d\psi \\ &= \log_2\left(\frac{e^{E_s/2N_0}}{I_0(E_s/2N_0)}\right), \end{aligned} \tag{116}$$

with $I_0(\cdot)$ the modified Bessel function of the first kind of order zero. For the slow-fading Rayleigh channel ($\zeta^2 = 0$) with *perfect* CSI, as follows from (111)-(113), we have

$$R_{0,1} = -\log_2 \frac{1}{2\pi} \int_{-\pi}^{\pi} \frac{1}{1 + E_s/N_0 \sin^2(\psi/2)} d\psi, \tag{117}$$

and for large enough E_s/N_0 this simplifies to

$$R_{0,1} = \frac{1}{2}\log_2(1 + E_s/N_0). \tag{118}$$

For the slow-fading Rician channel with *no* CSI, the limiting cutoff rate is similarly given by

$$R_{0,1} = -\log_2 \frac{1}{2\pi}\int_{-\pi}^{\pi} \exp\{-\frac{E_s}{4N_0} d'^2_{ME}(\psi)\}d\psi, \tag{119}$$

where

$$d'^2_{ME}(\psi) = \frac{\zeta^2 4\sin^2(\psi/2)}{1+\zeta^2+E_s/N_0}, \tag{120}$$

and we find

$$R_{0,1} = \log_2\Big(\frac{\exp\Big\{\frac{E_s}{2N_0}\frac{\zeta^2}{1+\zeta^2+E_s/N_0}\Big\}}{I_0(\frac{E_s}{2N_0}\frac{\zeta^2}{1+\zeta^2+E_s/N_0})}\Big). \tag{121}$$

Observe from (121), for infinite E_s/N_0, we have

$$R_{0,1} = \log_2\Big(\frac{e^{\zeta^2/2}}{I_0(\zeta^2/2)}\Big). \tag{122}$$

For constant-envelope modulation with *no* CSI and employing differential encoding/decoding, we have shown that the ML decoding rule can be approximated by the *linear* metric, and we now consider the limiting cutoff rate of the corresponding MDPSK scheme. Using a similar procedure as for the MPSK schemes, the limiting cutoff rate for MDPSK operating on the slow-fading Rician channel is given by

$$R'_{0,1} = -\log_2 \frac{1}{2\pi}\int_{-\pi}^{\pi} f'_d(\lambda^*,\psi)d\psi, \tag{123}$$

where, as shown in (A.22), the corresponding bound function on the pairwise error probability for large ζ^2 is given by

$$f'_d(\lambda^*,\psi) = \frac{1+\zeta^2+\frac{E_s}{N_0}(1-\rho)}{U}\exp\Big[\frac{-\frac{E_s}{8N_0}\zeta^2 d'^2_E(\psi)}{U}\Big], \tag{124}$$

with

$$U = 1+\zeta^2+\frac{E_s}{N_0}(1-\rho)+\Big[\frac{E_s}{4N_0}\rho - \frac{E_s}{16N_0}(1+\rho) - \frac{1+\zeta^2}{16}\Big]d'^2_E(\psi). \tag{125}$$

For large enough E_s/N_0 compared with $\zeta^2 (E_s/N_0 \gg \zeta^2)$ and $\rho \approx 1$, we have

$$R'_{0,1} = -\log_2 \frac{e^{-\zeta^2}}{2\pi}\int_{-\pi}^{\pi} \frac{d\psi}{1+\frac{(E_s/2N_0)}{1+\zeta^2}\sin^2(\psi/2)}, \tag{126}$$

or

$$R'_{0,1} = -\log_2 \frac{e^{\zeta^2}}{\sqrt{1 + \frac{E_s/2N_0}{1+\zeta^2}}}, \tag{127}$$

and, comparing (115) and (127), there is about 3dB SNR loss between the MPSK scheme with *perfect* CSI and the MDPSK scheme with *no* CSI. For the Rayleigh channel ($\zeta^2 = 0$), as shown in (A.26), the corresponding bounding function on the pairwise error probability is given by

$$f'_d(\lambda^*, \psi) = \frac{1}{\alpha \sin^2(\psi/2) + 1}, \tag{128}$$

where

$$\alpha = \rho^2 / \Big[((1-\rho) + N_0/E_s)((1+\rho) + N_0/E_s)\Big]. \tag{129}$$

For large enough E_s/N_0 and $\rho \approx 1$, the limiting cutoff rate simplifies to

$$R'_{0,1} = \frac{1}{2}\log_2\Big(1 + \frac{E_s}{N_0}\frac{1}{(2 + N_0/E_s)}\Big). \tag{130}$$

Comparing (118) and (130), there is again about 3dB SNR loss between MPSK with *perfect* CSI and MDPSK with *no* CSI when E_s/N_0 is large enough and $\rho \approx 1$.

Now we consider the limiting cutoff rate of QAM schemes for the slow-fading Rician channel with *perfect* CSI as well as the AWGN channel. For the QAM scheme, the optimum input distribution for the channel signaling alphabet $\tilde{s}(c_i)$ is not equiprobable as noted previously. Nevertheless, for tractability, we employ the equiprobable input distribution although the corresponding results are suboptimum. Then, the limiting cutoff rate for QAM is evaluated using a similar procedure as in the MPSK case where now we assume that the channel signaling alphabet $\tilde{s}(c_i) = x_i + jy_i$ is uniformly distributed in a square area such that the probability function is given by

$$Q^*(c_i) = p(x_i, y_i) = \frac{1}{4a^2};\ |x_i|, |y_i| < a, \tag{131}$$

and, for the conservation of the energy constraint, we impose the normalization such that

$$\int_{-a}^{a}\int_{-a}^{a} \frac{1}{4a^2}(x_i^2 + y_i^2)dx_i dy_i = 1, \tag{132}$$

with $a = \sqrt{3/2}$. Under the assumption of a uniform distribution, the limiting cutoff rate on the AWGN channel is then given by

$$R_{0,1} = -\log_2 \int_{-a}^{a}\int_{-a}^{a}\int_{-a}^{a}\int_{-a}^{a}\Big(\frac{1}{4a^2}\Big)^2 \exp\Big\{-\frac{E_s}{4N_0}d_E^2(c_i, \hat{c}_i)\Big\}dx_i d\hat{x}_i dy_i d\hat{y}_i, \tag{133}$$

with

$$d_E^2(c_i,\hat{c}_i) = |\tilde{s}(c_i) - \tilde{s}(\hat{c}_i)|^2 = (x_i - \hat{x}_i)^2 + (y_i - \hat{y}_i)^2. \tag{134}$$

Observe that from (133) with the substitution $x_i = 2ax_i' - a$, the limiting cutoff rate can be written as

$$R_{0,1} = -\log_2\left[\int_0^1\int_0^1 \exp\Big\{-\frac{3E_s}{2N_0}(x_i' - \hat{x}_i')^2\Big\}dx_i'd\hat{x}_i'\right]^2. \tag{135}$$

Let $x = |x_i' - \hat{x}_i'|$, so that the double intergration in (135) can be simplified to a single intergration, and we find

$$\begin{aligned} R_{0,1} &= -\log_2\left[\int_0^1 2(1-x)\exp\Big\{-\frac{3E_s}{2N_0}x^2\Big\}dx\right]^2 \\ &= -\log_2\Big[\sqrt{\frac{\pi}{3E_s/2N_0}}\mathrm{erf}\Big(\sqrt{\frac{3E_s}{2N_0}}\Big) - (\frac{3E_s}{2N_0})^{-1}(1-\exp\{\frac{3E_s}{2N_0}\})\Big]^2, \end{aligned} \tag{136}$$

where

$$\mathrm{erf}(x) = 1 - 2\mathcal{Q}(\sqrt{2}x) = \frac{2}{\sqrt{\pi}}\int_0^x e^{-t^2}dt. \tag{137}$$

Similarly, for the slow-fading Rician channel with *perfect* CSI, the limiting cutoff rate of the QAM scheme is given by

$$\begin{aligned} R_{0,1} &= -\log_2\int_{-a}^{a}\int_{-a}^{a}\int_{-a}^{a}\int_{-a}^{a}\Big(\frac{1}{4a^2}\Big)^2 E\Big\{\exp\{-\frac{E_s}{4N_0}|\tilde{z}_i|^2 d_E^2(c_i,\hat{c}_i)\}\Big\}dx_i d\hat{x}_i dy_i d\hat{y}_i \\ &= -\log_2 E\Big\{\int_{-a}^{a}\int_{-a}^{a}\int_{-a}^{a}\int_{-a}^{a}\Big(\frac{1}{4a^2}\Big)^2 \exp\{-\frac{E_s}{4N_0}|\tilde{z}_i|^2 d_E^2(c_i,\hat{c}_i)\}dx_i d\hat{x}_i dy_i d\hat{y}_i\Big\}, \end{aligned} \tag{138}$$

where the probability density function $p(|\tilde{z}_i|)$ is given in (11). Proceeding as in (133) and the sequel, it's easily seen that

$$\begin{aligned} R_{0,1} = -\log_2 E\Big\{\Big[\sqrt{\frac{\pi}{3|\tilde{z}_i|^2E_s/2N_0}}\mathrm{erf}(\sqrt{\frac{3|\tilde{z}_i|^2E_s}{2N_0}}) \\ -(\frac{3|\tilde{z}_i|^2E_s}{2N_0})^{-1}(1-\exp\{\frac{3|\tilde{z}_i|^2E_s}{2N_0}\})\Big]^2\Big\}. \end{aligned} \tag{139}$$

VI. Cutoff Rate Numerical Results:

In the previous sections, we provided expressions for the cutoff rate $R_{0,N}$ for several different modulation schemes on the slow-fading Rician channel under the assumption of *ideal* interleaving/deinterleaving of subsequences of length N. The evaluation of the cutoff

rate $R_{0,N}$ is extremely complicated for large N and, as a result, we only consider evaluation of $R_{0,N}$ for selected finite length N.

We first consider numerical evaluation of $R_{0,N}$ with *ideal* interleaving/deinterleaving when *perfect* CSI is available. Figure 4 shows the $R_{0,N}$ performance for MPSK as a function of E_b/N_0 with increasing values of N for both $B_0T_s = 0.1$ and $B_0T_s = 0.01$ on the Rayleigh channel. We have also illustrated the performance with *ideal* interleaving/deinterleaving of symbols ($N = 1$) indicated as a solid line for each value of alphabet size M, including the asymptotic value as $M \to \infty$. Observe that the $R_{0,N}$ performance with $N > 1$ is always inferior to the $R_{0,1}$ performance. Furthermore, in this case the performance of $R_{0,N}$ is a decreasing function of N and, although we expect that $R_{0,N}$ converges to a limiting value $R_{0,\infty}$ with *no* interleaving/deinterleaving as $N \to \infty$, we have been unable to evaluate this limiting value. Moreover, the $R_{0,N}$ performance is *decidedly* inferior for smaller values of normalized Doppler spread B_0T_s. If the fading component $\tilde{z}_i$ is constant for all i such that $B_0T_s = 0$, then, as shown in (73), for the Rayleigh channel we have $R_{0,\infty} = 0$ in which case the memoryless modulation scheme is useless without interleaving/deinterleaving. Therefore, when *perfect* CSI is available it is best to employ interleaving/deinterleaving strategies on individual symbols.

Now consider the performance of memoryless modulation with *ideal* interleaving/deinterleaving of symbols ($N = 1$) only. We first consider the performance of MPSK when *perfect* CSI is available. In this case the cutoff rates are independent of the Doppler spread B_0T_s. Figure 5 shows the cutoff rate performance with *perfect* CSI operating on the slow-fading Rician channel ($\zeta^2 = 10$dB), the slow-fading Rayleigh channel ($\zeta^2 = 0$), as well as the AWGN channel ($\zeta^2 = \infty$). Observe from Fig. 5 the slow convergence of $R_{0,1}$ to the maximum value $\log_2 M$ for small values of ζ^2. Furthermore, for any integer throughput m, in bits/channel use, most of the coding gain, which is possible over a *baseline* uncoded system operating at the same throughput, can be obtained by employing a signaling alphabet of size $M = 2^{m+1}$ and using a rate $R_c = m/m + 1$ code. This is, of course, a known result for the AWGN channel [15].

We now compare the performance of QAM with MPSK in terms of the cutoff rate parameter $R_{0,1}$ in Fig.'s 6 and 7. Here, we assume that *ideal* interleaving/deinterleaving of symbols ($N = 1$) and *perfect* CSI are employed. Figure 6 demonstrates, as expected, that

the cutoff rate for QAM is greater than that of a comparable MPSK with the same alphabet size on the AWGN channel and, moreover, that this difference increases with increasing alphabet size. In Fig. 7, QAM performance is still better than that of MPSK on the Rayleigh fading channel (ζ^2=0) although, as we see in comparing Fig.'s 6 and 7, the difference in $R_{0,1}$ between the two schemes is not as pronounced as the ratio of specular-to-diffuse energy ζ^2 is decreased.

Next, we consider numerical evaluation of $R_{0,N}$ for the Rician fading channel which has $\zeta^2 = 10\text{dB}$ and $B_0T_s = 0.01$ with *ideal* interleaving/deinterleaving of subsequences of length N when CSI is not available. Figure 8 shows the $R_{0,N}$ performance for QPSK as a function of E_b/N_0 with increasing values of N for $B_0T_s = 0.01$. For comparison, we also provide the $R_{0,1}$ performance for the case of *perfect* CSI as well as the $R_{0,1}$ performance for differential QPSK (DQPSK) with *no* CSI. As shown in this figure, for small E_b/N_0 ($< 6\text{dB}$), the cutoff rate performance for $N = 1$ is greater than the other cases considered ($N > 1$), and, as E_b/N_0 increases, the length N that achieves the optimum $R_{0,N}$ performance increases. For large enough E_b/N_0, the cutoff rate performance $R_{0,N}$ for QPSK with any N is inferior to the cutoff rate $R'_{0,1}$ for the DQPSK scheme. Hence, *ideal* interleaving/deinterleaving by symbols ($N = 1$) should be employed for small E_b/N_0 in this special case, and the differential MPSK scheme should be considered for larger values of E_b/N_0.

Now consider numerical evaluation of $R_{0,N}$ for the Rayleigh channel with *ideal* interleaving/deinterleaving of subsequences of length N when CSI is not available as illustrated in Fig.'s 9 and 10. Figure 9 shows the $R_{0,N}$ performance for QPSK as a function of E_b/N_0 with increasing values of N for $B_0T_s = 0.01$. For comparison, we also provide the $R_{0,1}$ performance for the case of *perfect* CSI as well as the $R_{0,1}$ performance for DQPSK with *no* CSI. Again, as increases E_b/N_0, the length N that achieved the optimum $R_{0,N}$ performance increases. Moreover, as shown and discussed in (89), the cutoff rate $R'_{0,N}$ for MPSK with differential encoding is greater than $R_{0,N+1}$ for MPSK for $N = 1, 2, \cdots$, and hence differential encoding should be employed for MPSK on the Rayleigh channel. Figure 10 shows the $R'_{0,N}$ performance for QPSK with differential encoding on the Rayleigh channel with $B_0T_s = 0.01$. Observe that the $R'_{0,N}$ performance with $N > 1$ is always inferior to the $R'_{0,1}$ performance. In this case the performance of $R'_{0,N}$ is a decreasing function of N. According to results in (89) and this figure, when CSI is not available on the Rayleigh channel, it is best to employ

the differential encoding/decoding technique with interleaving/deinterleaving strategies on a symbol-by-symbol basis ($N = 1$).

In Fig. 11, assuming again that *ideal* interleaving/deinterleaving of symbols ($N = 1$) is employed, we have plotted cutoff rate curves for MPSK with *no* CSI on the slow-fading Rician channels with the ratio of specular-to-diffuse energy $\zeta^2 = 10$dB, 15dB and $\zeta^2 = \infty$ (AWGN). For a fixed ζ^2 the $R_{0,1}$ curves become indistinguishable as M increases. Notice the significant degradation relative to the corresponding results for *perfect* CSI in Fig. 5. This degradation is particularly pronounced for larger values of M. Indeed, for $M > 4$ the *limiting* value of $R_{0,1}$ is significantly less than $\log_2 M$ for finite ζ^2. This is consistent with observations concerning the existence of a maximum usable operating rate as defined by (84) and the sequel and illustrated in Fig. 2. Nevertheless, we see that for small enough throughputs, $m \leq 3$ say, it's possible, as in the case of *perfect* CSI, to realize substantial coding gains relative to the uncoded baseline system by again doubling the signaling alphabet and employing an $R_c = m/m + 1$ code. However, for large throughputs there is little to be gained in the presence of severe fading by employing such a strategy when *no* CSI is available.

Next, for the case of *no* CSI, we present results on the performance of MDPSK in terms of the cutoff rate. As shown in Section III.3, an approximate ML decoding metric for MDPSK schemes is the simple *linear* metric when the fading is slow enough ($\rho \approx 1$) or the ratio of specular-to-diffuse energy is small enough ($\zeta^2 \approx 0$). Figure 12 shows the comparison of cutoff rates for coherent MPSK schemes and MDPSK schemes operating on the AWGN channel and, as expected, there is about a 3dB SNR difference between coherent MPSK schemes and MDPSK schemes. For the case of large ζ^2, we expect that the performance of MPSK with *no* CSI is superior to the performance of MDPSK.

In Fig.'s 13 and 14, we illustrate the limiting performance of R_0 for MDPSK for large alphabet size M ($M \rightarrow \infty$) and for different values of B_0T_s. For comparison purposes we have also included the limiting performance of MPSK for both the cases of *perfect* CSI and *no* CSI. Figure 13 shows the limiting performance of MDPSK for both $B_0T_s = 0.1$ and $B_0T_s = 0.01$ operating on the Rician fading channel ($\zeta^2 = 10$dB). For the case of *no* CSI, the performance of MDPSK for both $B_0T_s = 0.1$ and $B_0T_s = 0.01$ is superior to the performance of MPSK for large E_b/N_0. However, the performance of MDPSK is inferior to the corresponding performance of MPSK for small E_b/N_0 (< 7dB). Moreover, the limiting

performance of MDPSK improves with smaller values of normalized Doppler spread, B_0T_s. Similarly, Fig. 14 shows the limiting performance of MDPSK for both $B_0T_s = 0.1$ and $B_0T_s = 0.01$ operating on the Rayleigh fading channel ($\zeta^2 = 0$). We have also included the limiting performance of MPSK with *perfect* CSI. As can be seen from (121), the limiting performance $R_{0,1}$ of MPSK with *no* CSI is always zero for $\zeta^2 = 0$. Therefore, for the case of *no* CSI, the MPSK scheme is useless, and one should use MDPSK instead of MPSK. According to Fig.'s 13 and 14, the performance of MDPSK is improved when B_0T_s is reduced, and the performance of MDPSK is far superior to the performance of MPSK with *no* CSI when the fading is slow enough and SNR is large.

VII. Summary and Conclusions:

We have provided explicit and comprehensive evaluation of the cutoff rate for memoryless modulation on the slow-fading Rician channel both with *perfect* and *no* CSI when *ideal* interleaving/deinterleaving is used. These cutoff rate results should prove useful in assessing modulation/coding tradeoffs on representative slow-fading Rician channels. For the case of *no* interleaving/deinterleaving, the evaluation of the cutoff rate is extremely complicated, and we only consider the value $R_{0,N}$ for finite block length N instead of the limiting value R_0 as $N \to \infty$. According to cutoff rate results presented here, for the case of *perfect* CSI, it is generally best to employ interleaving/deinterleaving strategies, and the QAM scheme performs considerably better than the MPSK scheme. For the case of *no* CSI, we evaluated the cutoff rate for constant-envelope modulation only with *ideal* interleaving/deinterleaving, and provided cutoff rate results for both MPSK and MDPSK for which the ML decoding metric is approximated by the sum of the individual *branch metrics*. Moreover, employing *ideal* interleaving/deinterleaving, we demonstrated that, for the case of *no* CSI, the cutoff performance of MDPSK is significantly superior to that of MPSK when the fading is slow enough and ζ^2 is small enough.

Appendix A

Chernoff Bounds on Pairwise Sequence Error Probability

A.1. M-ary Differential PSK

We suppose that $\mathbf{c}^N = (c_0, c_1, c_2, \cdots, c_N)$ be the transmitted sequence of length N at the output of the differential encoder with input sequence $\{c'_n\}$ such as $c_i = modulo(\sum_{n=0}^{i} c'_n, M)$. Then, with $\tilde{\mathbf{r}}^N = (\tilde{r}_1, \tilde{r}_2, \ldots, \tilde{r}_N)$ the demodulator channel output sequence, a sequence $\hat{\mathbf{c}}'^N$ is chosen over the sequence $\mathbf{c}'^N$ if

$$m_{ML}(\tilde{\mathbf{r}}^N; \hat{\mathbf{c}}'^N) > m_{ML}(\tilde{\mathbf{r}}^N; \mathbf{c}'^N) \tag{A.1}$$

where $m_{ML}(\tilde{\mathbf{r}}^N; \mathbf{c}'^N)$ is corresponding ML metric which is given in (39). The previous received signal is available for use in differentially coherent detection, and ML metric is approximated to a Gaussian metric as shown in Section III.3 and is given in (49) such as

$$m(\tilde{r}_i; \tilde{r}_{i-1}, c'_i) = Re\{\tilde{r}_i \tilde{r}^*_{i-1} e^{-j2\pi c'_i/M}\}. \tag{A.2}$$

By straight forward Chernoff bounding techniques, we obtain

$$\begin{aligned} Pr\{\mathbf{c}'^N \rightarrow \hat{\mathbf{c}}'^N \mid \mathbf{c}'^N\} &\leq \min_{\lambda \geq 0} E\{e^{\lambda[m(\tilde{\mathbf{r}}^N; \hat{\mathbf{c}}'^N) - m(\tilde{\mathbf{r}}^N; \mathbf{c}'^N)]} \mid \mathbf{c}'^N\} \\ &= \min_{\lambda \geq 0} \prod_{i=1}^{N} E\{e^{\lambda[m(\tilde{r}_i; \hat{c}'_i, \tilde{r}_{i-1}) - m(\tilde{r}_i; c'_i, \tilde{r}_{i-1})]} \mid c'_i, \tilde{r}_{i-1}\} \end{aligned} \tag{A.3}$$

where the last equality follows the assumed independence of the components of $\{\tilde{r}_i \tilde{r}^*_{i-1}\}$ given $\{c'_i\}$. The conditional expectations in (A.3) can be expressed as

$$E\{e^{\lambda[m(\tilde{r}_i; \hat{c}'_i, \tilde{r}_{i-1}) - m(\tilde{r}_i; c'_i, \tilde{r}_{i-1})]} \mid c'_i, \tilde{r}_{i-1}\} = E\{e^{\lambda Y_i} \mid c'_i, \tilde{r}_{i-1}\} \tag{A.4}$$

where $Y_i = Re\{\tilde{Y}_i\};\ i = 1, 2, ..., N$ with

$$\tilde{Y}_i = \tilde{r}_i \tilde{r}^*_{i-1}[e^{-j2\pi \hat{c}'_i/M} - e^{-j2\pi c'_i/M}];\ i = 1, 2, ..., N. \tag{A.5}$$

Assuming the first-order Markov process channel, with the relation between two fading components $\tilde{z}_i$ and $\tilde{z}_{i-1}$ in (36), $\tilde{Y}_i$ be written as

$$\tilde{Y}_i = \Big((\rho \tilde{z}_{i-1} + (1-\rho)\Gamma + \sqrt{1-\rho^2}\tilde{w}_i)e^{-j2\pi c_i/M} + \frac{1}{\sqrt{E_s}}\tilde{n}_i\Big)\tilde{r}^*_{i-1}[e^{-j2\pi \hat{c}'_i/M} - e^{-j2\pi c'_i/M}]$$

$$= \left(\rho\tilde{r}_{i-1}e^{-j2\pi c_i'/M} - \rho e^{-j2\pi c_i'/M}\frac{\tilde{n}_{i-1}}{\sqrt{E_s}} + \Gamma(1-\rho)e^{-j2\pi c_i/M} + e^{-j2\pi c_i/M}\tilde{w}_i + \frac{1}{\sqrt{E_s}}\tilde{n}_i\right)\cdot \tilde{r}_{i-1}^*[e^{-j2\pi\hat{c}_i'/M} - e^{-j2\pi c_i'/M}]. \quad (A.6)$$

The jointly Gaussian distribution density function of $\tilde{n}_i$ is given by

$$P(\tilde{n}_i/\sqrt{E_s} \mid \tilde{r}_i) = \frac{1}{\pi(1-\kappa^2)N_0/E_s}\exp\left\{\frac{-|\frac{\tilde{n}_i}{\sqrt{E_s}} - \frac{\kappa}{\sigma_{\tilde{r}_i}}\sqrt{\frac{N_0}{E_s}}(\tilde{r}_i - \Gamma e^{-j2\pi c_i})|^2}{(1-\kappa^2)N_0/E_s}\right\}, \quad (A.7)$$

where the variance of $\tilde{r}_i$ is given by

$$\sigma_{\tilde{r}_i}^2 = 2\sigma_a^2 + N_0/E_s, \quad (A.8)$$

and the covariance of $\tilde{n}_i/\sqrt{E_s}$ and $\tilde{r}_i$ is given by

$$\kappa = \frac{1}{\sqrt{1+2\sigma_a^2 E_s/N_0}}. \quad (A.9)$$

Then the quantity $\tilde{Y}_i$ is a conditionally complex Gaussian variate given c_i' and $\tilde{r}_{i-1}$ with the conditional mean value

$$\begin{aligned} m_{Y_i} &= Re\{E\{\tilde{Y}_i \mid c_i', \tilde{r}_{i-1}\}\} \\ &= \frac{-\sigma_a^2\rho|\tilde{r}_{i-1}|^2 d_E^2(c_i', \hat{c}_i')}{2\sigma_a^2 + N_0/E_s} + \frac{\Gamma N_0/E_s + \Gamma 2\sigma_a^2(1-\rho)}{2\sigma_a^2 + N_0/E_s} \\ &\quad \cdot Re\{e^{-j2\pi c_i/M}\tilde{r}_{i-1}^*[e^{-j2\pi\hat{c}_i'/M} - e^{-j2\pi c_i'/M}]\} \end{aligned} \quad (A.10)$$

and the variance

$$\begin{aligned} \sigma_{Y_i}^2 &= \frac{1}{2}var\{\tilde{Y}_i \mid c_i, \tilde{r}_{i-1}\} \\ &= \frac{4\sigma_a^4(1-\rho^2) + 4\sigma_a^2 N_0/E_s + (N_0/E_s)^2}{2(2\sigma_a^2 + N_0/E_s)}|\tilde{r}_{i-1}|^2 d_E^2(c_i', \hat{c}_i') \end{aligned} \quad (A.11)$$

where $d_E^2(c_i', \hat{c}_i') = 4\sin^2(\pi(c_i' - \hat{c}_i')/M)$ is the normalized Euclidean distance between signaling elements transmitted during the i'th branch. Finally, the conditional expectation on the righthand side of (A.4) is evaluated as

$$E\{e^{\lambda Y_i} \mid c_i', \tilde{r}_{i-1}\} = \psi_{Y_i}(u)|_{u=\lambda/j} \quad (A.12)$$

where

$$\psi_{Y_i}(u) = \exp\{jum_{Y_i} - \frac{1}{2}u^2\sigma_{Y_i}^2\} \quad (A.13)$$

is the conditional characteristic function of Y_i, which is given in [1]. Thus, we have from (A.12) with (A.3) that

$$Pr\{\mathbf{c}'^N \to \hat{\mathbf{c}}'^N \mid \mathbf{c}'^N\} \leq \prod_{i=1}^{N} \min_{\lambda \geq 0} E\Big\{\exp\{\lambda m_{Y_i} + \frac{1}{2}\lambda^2 \sigma_{Y_i}^2\}\Big\}, \tag{A.14}$$

and the expectation in (A.14) be evaluated as follows,

$$\begin{aligned} E\{\exp\{\lambda m_{Y_i} + \frac{1}{2}\lambda^2 \sigma_{Y_i}^2\}\} &= \int_{-\infty}^{\infty} \exp\{\lambda m_{Y_i} + \frac{1}{2}\lambda^2 \sigma_{Y_i}^2\} p(\tilde{r}_{i-1}|c_{i-1}) d\tilde{r}_{i-1} \\ &= \frac{1}{A(\lambda, E_s/N_0, \rho)} \exp\Big\{\frac{B(\lambda, E_s/N_0, \rho)}{A(\lambda, E_s/N_0, \rho)}\Big\} \end{aligned} \tag{A.15}$$

where

$$\begin{aligned} A(\lambda, E_s/N_0, \rho) &= 1 + \lambda\rho\sigma_a^2 d_E^2(c_i', \hat{c}_i') \\ &\quad -\frac{\lambda^2}{4}(2\sigma_a^2(1-\rho) + N_0/E_s)(2\sigma_a^2(1+\rho) + N_0/E_s) d_E^2(c_i', \hat{c}_i'), \end{aligned} \tag{A.16}$$

and

$$B(\lambda, E_s/N_0, \rho) = -\frac{\lambda}{2}\Gamma^2 d_E^2(c_i', \hat{c}_i') + \frac{\lambda^2}{2}\Gamma^2(2\sigma^2(1-\rho) + N_0/E_s) d_E^2(c_i', \hat{c}_i'). \tag{A.17}$$

Now we choose λ^* as the optimum value of λ to minimize $E\{e^{\lambda Y_i}|c_i'\}$.

On the slow-fading Rician channel with large $\zeta^2$and large E_s/N_0, $A(\lambda, E_s/N_0, \rho)$ changes much slower than $B(\lambda, E_s/N_0, \rho)$ about the variable λ, and the optimum value of λ can be approximated by

$$\frac{\partial B(\lambda^*, E_s/N_0, \rho)}{\partial \lambda^*} = 0, \tag{A.18}$$

and we find λ^* as

$$\lambda^* = \frac{1}{2(2\sigma_a^2(1-\rho) + N_0/E_s)}. \tag{A.19}$$

Substituting this optimizing value λ^* into (A.15), we find

$$E\{e^{\lambda Y_i}|c_i'\} = \frac{1 + \frac{2E_s}{N_0}\sigma_a^2(1-\rho)}{V} \exp[\frac{-\frac{E_s}{8N_0}\Gamma^2 d_E^2(c_i', \hat{c}_i')}{V}], \tag{A.20}$$

where

$$V = 1 + \frac{E_s}{N_0}2\sigma_a^2(1-\rho) + \frac{E_s}{4N_0}2\sigma_a^2\rho d_E^2(c_i', \hat{c}_i') - \frac{1}{16}(\frac{E_s}{N_0}2\sigma_a^2(1+\rho) + 1) d_E^2(c_i', \hat{c}_i'). \tag{A.21}$$

The expression in (A.20) can be written with ζ^2 as

$$E\{e^{\lambda Y_i}|c_i'\} = \frac{1+\zeta^2+\frac{E_s}{N_0}(1-\rho)}{U}\exp\left[\frac{-\frac{E_s}{8N_0}\zeta^2 d_E^2(c_i', \hat{c}_i')}{U}\right] \tag{A.22}$$

where

$$U = 1+\zeta^2+\frac{E_s}{N_0}(1-\rho)+\left[\frac{E_s}{4N_0}\rho - \frac{E_s}{16N_0}(1+\rho) - \frac{1+\zeta^2}{16}\right]d_E^2(c_i', \hat{c}_i'). \tag{A.23}$$

On the slow-fading Rayleigh channel, $B(\lambda, E_s/N_0, \rho)$ is always zero, and then the optimum value of λ can be evaluated by

$$\frac{\partial A^{-1}(\lambda^*, E_s/N_0, \rho)}{\partial \lambda^*} = 0, \tag{A.24}$$

and we find λ^* as

$$\lambda^* = \rho/\Big[((1-\rho)+N_0/E_s)((1+\rho)+N_0/E_s)\Big]. \tag{A.25}$$

Substituting this optimizing value λ^* into (A.15), we find

$$E\{e^{\lambda Y_i}|c_i'\} = \frac{((1-\rho)+N_0/E_s)((1+\rho)+N_0/E_s)}{\rho^2 d_E^2(c_i', \hat{c}_i')/4 + ((1-\rho)+N_0/E_s)((1+\rho)+N_0/E_s)}. \tag{A.26}$$

Appendix B

Evaluation of Cutoff Rate $R_{0,\infty}$ for Rayleigh Channel with $\rho = 1$

Here, we evaluate the cutoff rate $R_{0,N}$ for the case of *no* interleaving/deinterleaving on the Rayleigh channel with $\rho = 1$ when N goes to infinity. From (72), we have

$$R_{0,N} = -\log \sqrt[N]{\int_0^1 \Big(\frac{1}{M^2}\sum_{c_i,\hat{c}_i} u^{\frac{E_s}{4N_0}d_E^2(c_i,\hat{c}_i)}\Big)^N du}. \tag{B.1}$$

The bound of integrand appearing in (B.1) can be given by

$$\int_0^1 \Big(u^{\frac{E_s}{4N_0}d_{E,max}^2}\Big)^N du \le \int_0^1 \Big(\frac{1}{M^2}\sum_{c_i,\hat{c}_i} u^{\frac{E_s}{4N_0}d_E^2(c_i,\hat{c}_i)}\Big)^N du \le \int_0^1 \Big(u^{\frac{E_s}{4N_0}d_{E,min}^2}\Big)^N du, \tag{B.2}$$

where, for any $c_i, \hat{c}_i \in 0, \cdots, M-1$,

$$d_{E,max}^2 = \max d_E^2(c_i, \hat{c}_i) \tag{B.3}$$

and

$$d_{E,min}^2 = \min d_E^2(c_i, \hat{c}_i) = 0. \tag{B.4}$$

After some algebra, the bound in (B.2) can be expressed as

$$1 \le \int_0^1 \Big(\frac{1}{M^2}\sum_{c_i,\hat{c}_i} u^{\frac{E_s}{4N_0}d_E^2(c_i,\hat{c}_i)}\Big)^N du \le \frac{1}{N\frac{E_s}{4N_0}d_{E,max}^2 + 1}. \tag{B.5}$$

For finite value α, we can easily evaluate following limitation

$$\lim_{N\to\infty} \sqrt[N]{\frac{1}{N\alpha+1}} = 1. \tag{B.6}$$

Substitution this value to (B.5), for the finite E_s/N_0, we have

$$\lim_{N\to\infty} \sqrt[N]{\int_0^1 \Big(\frac{1}{M^2}\sum_{c_i,\hat{c}_i} u^{\frac{E_s}{4N_0}d_E^2(c_i,\hat{c}_i)}\Big)^N du} = 1, \tag{B.7}$$

and then

$$\lim_{N\to\infty} R_{0,N} = -\log_2 1 = 0. \tag{B.8}$$

References

[1] J. W. Modestino, K. Park and S. N. Hulyalkar, "Trellis-Coded MPSK Operating on the Slow-Fading Rician Channel," submitted to IEEE Trans. Inf. Theory.

[2] K. Park, "Trellis-Coded Modulation on a Slow-Fading Rician Channel," M. S. Thesis, Dept. Elect., Comput., Syst. Engg., Rensselaer Polytechnic Institute, Troy, NY, May 1991.

[3] J. W. Modestino, "Cutoff Rate for Phase-Only Modulation on a Slow-Fading Rician Channel," ECSE Department Report, RPI, Troy, NY-12180, March 1991.

[4] J. W. Modestino, "Use of the EM Algorithm for Incorporating Channel State Information into Decoding Procedures," ECSE Department Report, RPI, Troy, NY, Feb. 1992.

[5] J. W. Modestino, "Likelihood Functional for the Detection of a Known Signal in a Slow-Fading Rician Channel," ECSE Department Report, RPI, Troy, NY-12180, 1991.

[6] J. W. Modestino and S. Y. Mui, "Convolutional Code Performance on the Rician Fading Channel," IEEE Trans. Comm.Vol. COM-24, pp. 592-606, June 1976.

[7] J. L. Massey, "Coding and Modulation in Digital Communications," *Proc. Int. Zurich Seminar on Digital Communications*, Zurich, Switzerland, pp. E2(1)-E2(4), 1974.

[8] J. M. Wozencraft, I. M. Jacobs, "Principles of Communication Engineering," Wiley, New York, 1965.

[9] R. G. Gallager, "Information Theory and Reliable Communication," Wiley, New York, 1968.

[10] R. Blahut, "Theory and Practice of Error Control Codes," Addison- Wesley Pub. Co., Reading, MA, 1983.

[11] R. J.McEliece and W. E. Stark, "Channels with Block Interference," IEEE Trans. on Inform. Theory, Vol. IT-30, pp. 44-53, Jan. 1984.

[12] D. Divsalar and M. K. Simon, "The Design of Trellis-Coded MPSK for Fading Channels: Performance Criteria," IEEE Trans. Comm.Vol. COM-36, pp. 1004-1012, Sep. 1988.

[13] D. Divsalar and M. K. Simon, "The Design of Trellis-Coded MPSK Modulation Fading Channels: Set Partitioning for Optimum Code Design," IEEE Trans. Comm.Vol. COM-36, pp. 1013-1021, Sep. 1988.

[14] D. Divsalar, M. K. Simon, and T. Jedrey, "Trellis Coding Techniques for Mobile Communications," IEEE Military Communications Conference vol. 2, pp. 653-659, San Diego, CA, 1988.

[15] G. Ungerboeck, "Channel Coding with multilevel/phase signals", IEEE Trans. Inf. Theory, Vol. IT-28, pp. 55-67, Jan. 1982.

[16] H. L. VanTrees, *"Detection, Estimation and Modulation Theory: Part I,"* John Wiley and Sons, New York, 1968.

[17] K. Leeuwin, J. C. Belfiore, and G. Kawas Kaleh, "Chernoff Bound of Trellis-Coded Modulation Over Correlated Fading Channels," IEEE Trans. Comm., Vol. COM-42, pp. 2506-2510, Aug. 1994.

[18] K. Leeuwin-Boulle, and J. C. Belfiore, "The cutoff Rate of Time Correlated Fading Channels," IEEE Trans. Inf. Theory, Vol. IT-39, pp. 612-617, Mar. 1993.

[19] H. Ho and D. Fung, "Error Performance of Multiple-Symbol Differential Detection of PSK Signals Transmitted Over Correlated Rayleigh Fading Channels," IEEE Trans. Comm., Vol. COM-40, pp. 1566-1569, Oct. 1992.

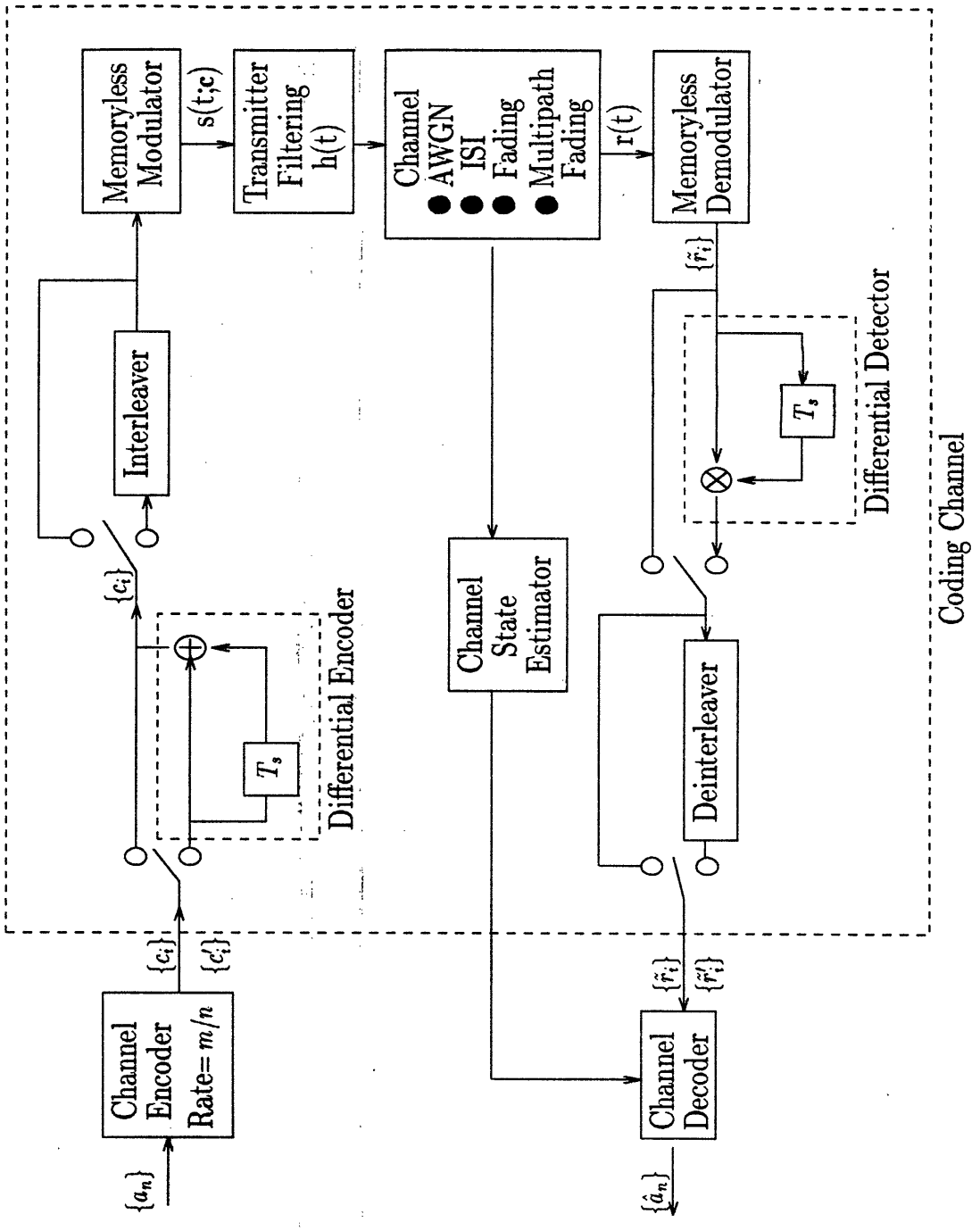

Figure 1
Block Diagram of a Generic Communication System.

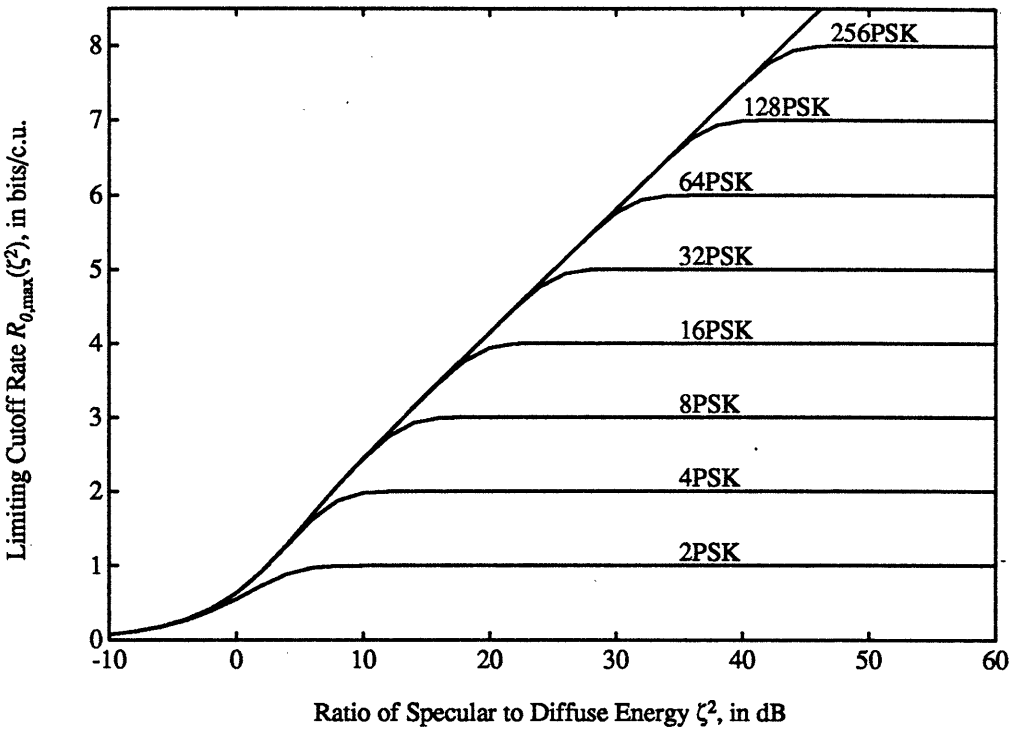

Figure 2
Behavior of Limiting Cutoff Rate $R_{0,\max}(\zeta^2)$ as a Function of ζ^2
for Different Alphabet size; M, for Ideal Interleaved Rician Channel With No CSI.

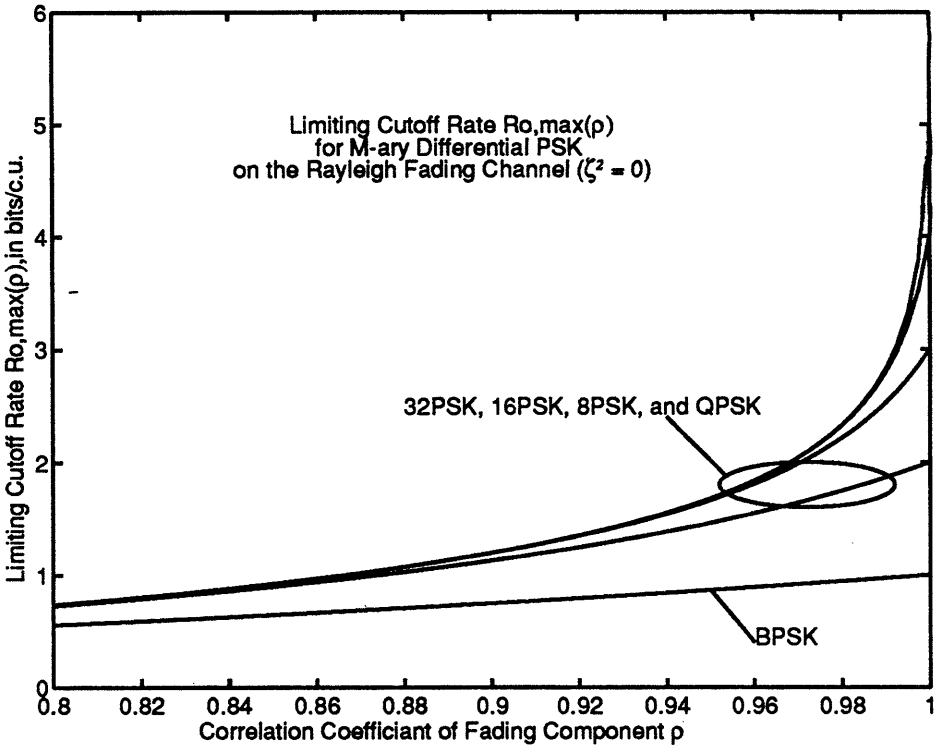

Figure 3
Behavior of Limiting Cutoff Rate $R_{0,\max}(\rho)$ as a Function of ρ
for MDPSK Schemes on the Rayleigh Fading Channel
With Ideal Interleaving/Deinterleaving of Symbols ($N = 1$).

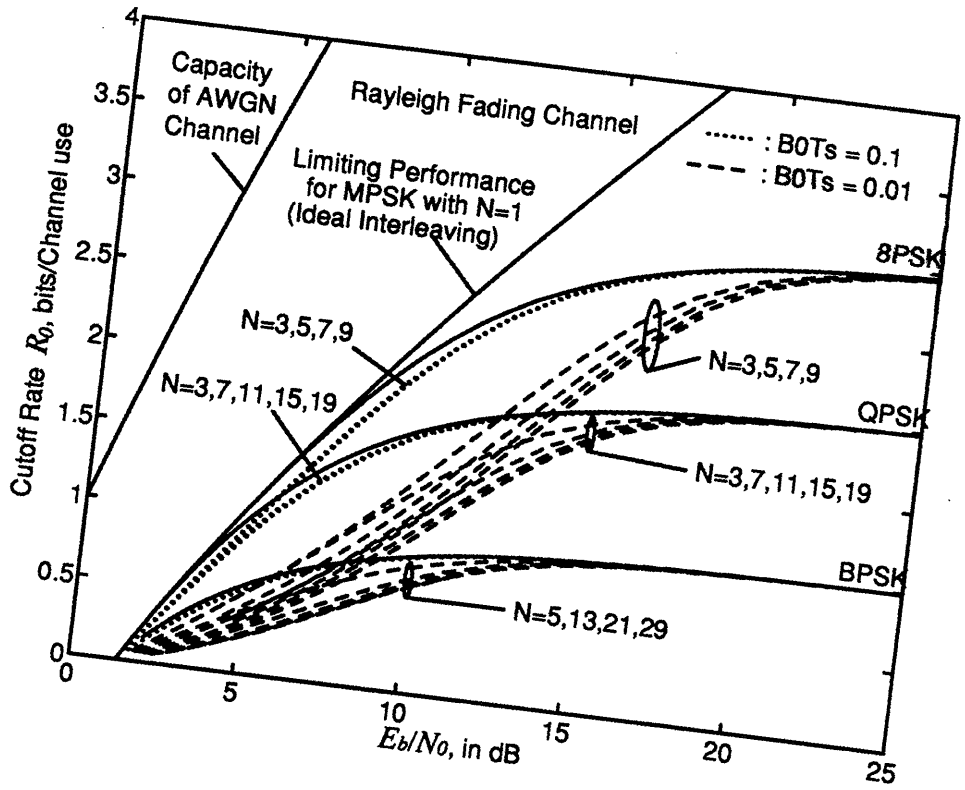

Figure 4
Cutoff Rate $R_{0,N}$ Performance for MPSK Signaling
on the Rayleigh Fading Channel With Perfect CSI
and With Ideal Interleaving/Deinterleaving of Subsequences of Length N.

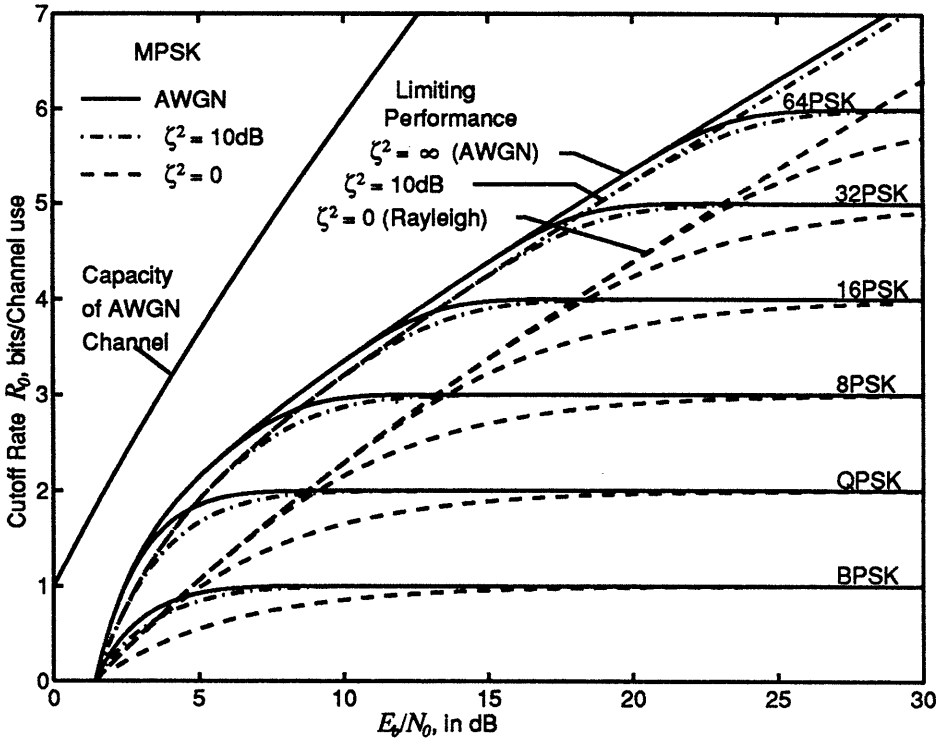

Figure 5
Comparison of Cutoff Rate $R_{0,1}$ Performance for MPSK Signaling on the Rician Channel for Selected values of ζ^2 With *Perfect* CSI and *Ideal* Interleaving/Deinterleaving on a Symbol Basis ($N = 1$).

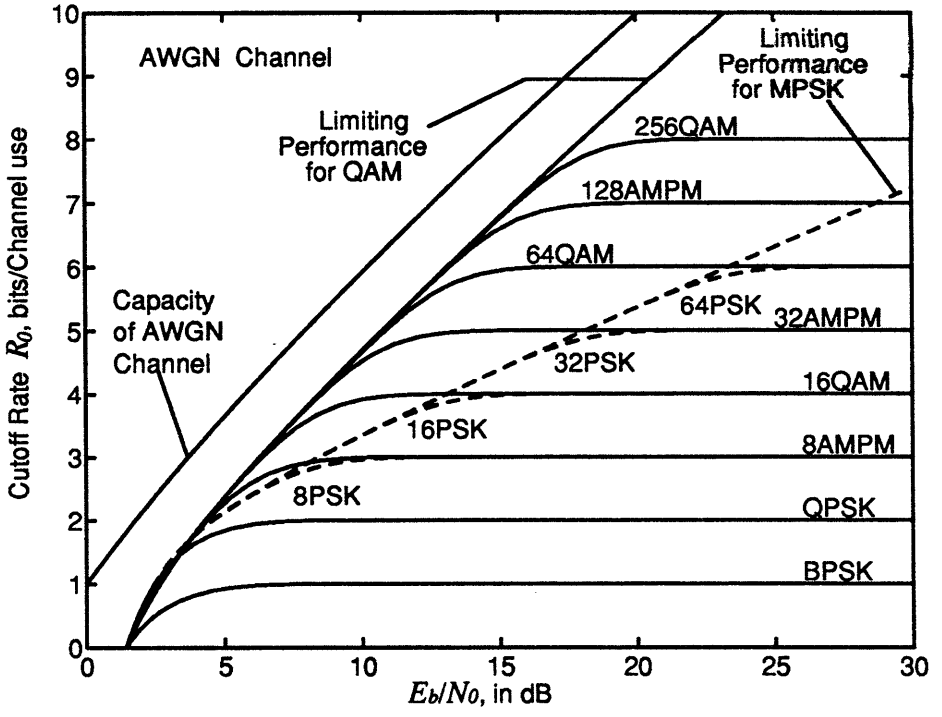

Figure 6
Comparison of Cutoff Rate $R_{0,1}$ Performance
for QAM and MPSK Signaling on the AWGN Channel.

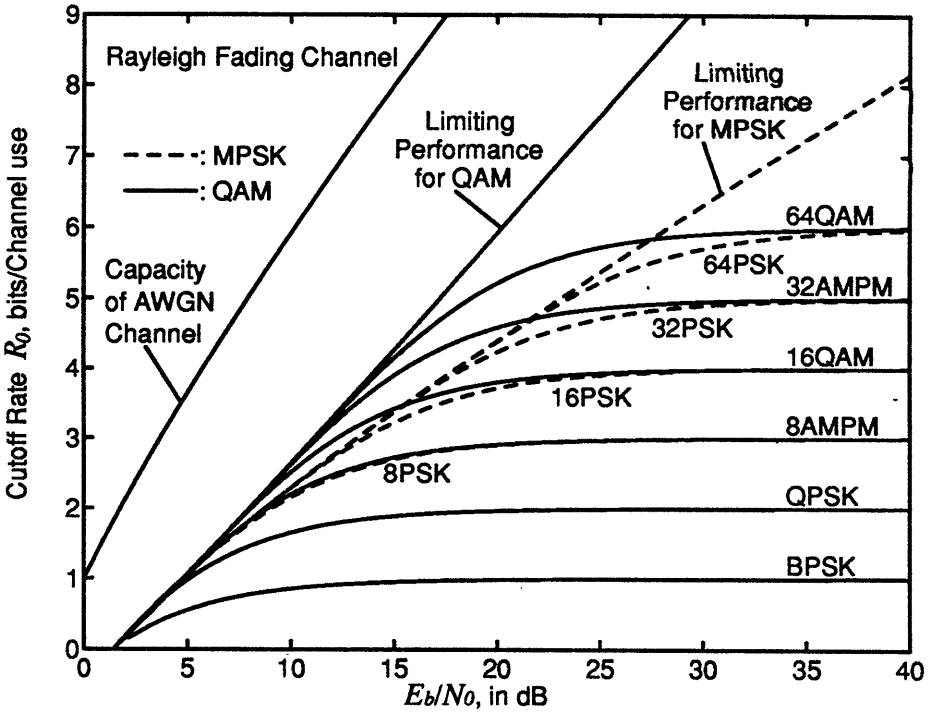

Figure 7
Comparison of Cutoff Rate $R_{0,1}$ Performance for QAM and MPSK Signaling on the Rayleigh Channel with *Perfect* CSI and *Ideal* Interleaving/Deinterleaving on a Symbol Basis ($N = 1$).

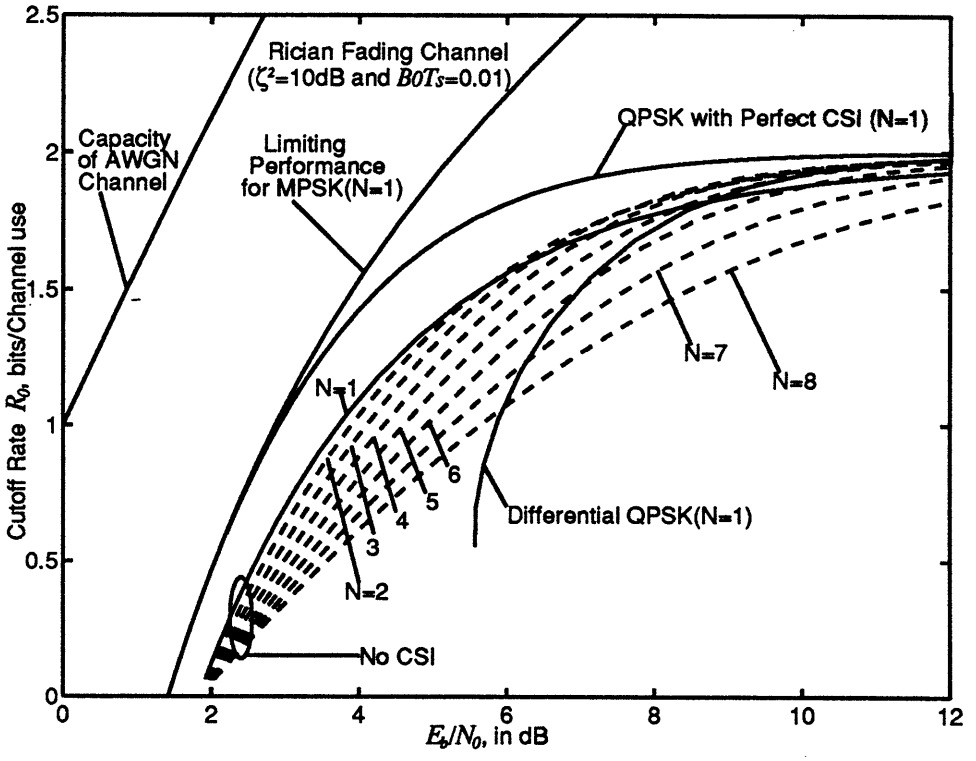

Figure 8
Cutoff Rate $R_{0,N}$ Performance for QPSK Signaling
on the Rician Fading Channel ($\zeta^2 = 10$dB) With No CSI
and With Ideal Interleaving/Deinterleaving of Subsequences of Length N.

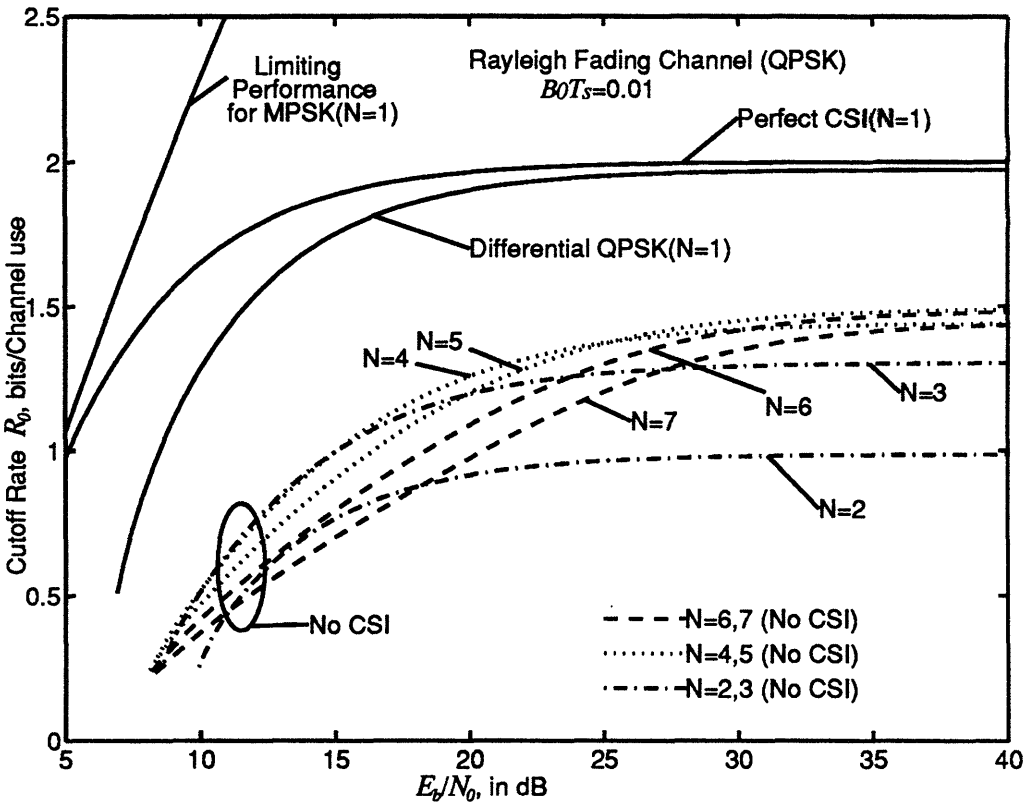

Figure 9
Cutoff Rate $R_{0,N}$ Performance for QPSK Signaling
on the Rayleigh Fading Channel With No CSI and With Ideal
Interleaving/Deinterleaving of Subsequences of Length N.

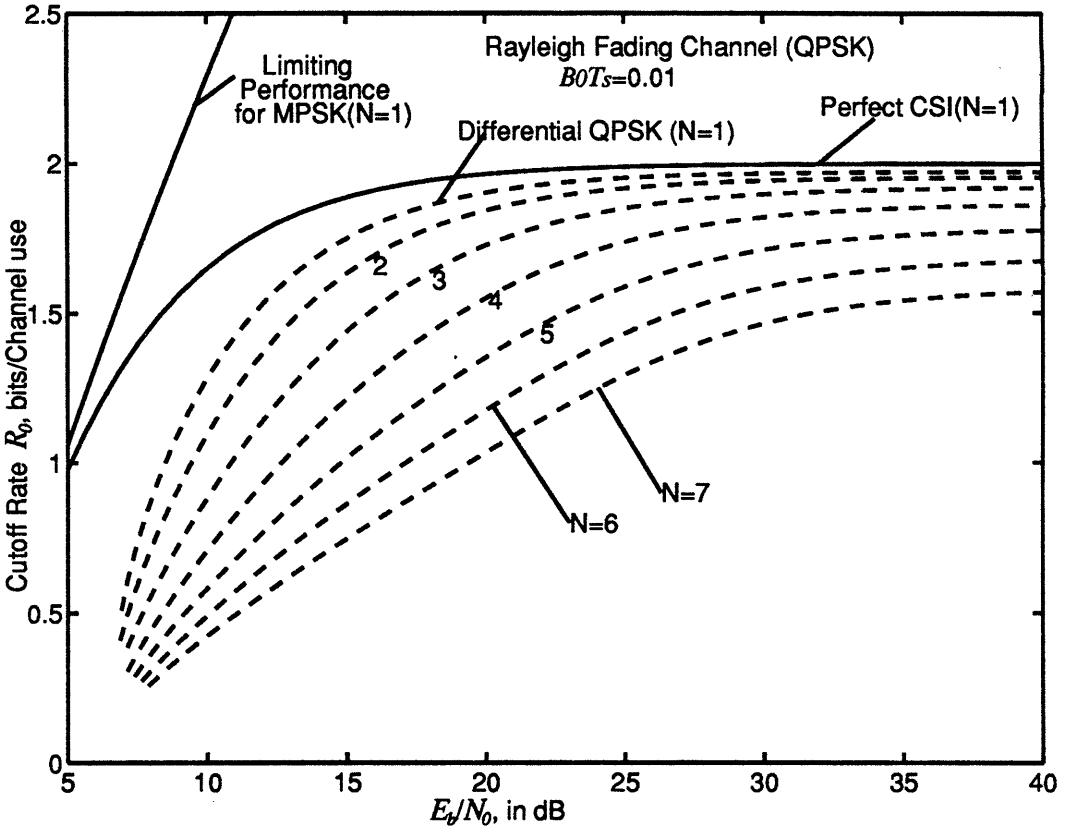

Figure 10
Cutoff Rate $R'_{0,N}$ Performance for Differential QPSK Signaling on the Rayleigh Fading Channel With No CSI and With Ideal Interleaving/Deinterleaving of Subsequences of Length N.

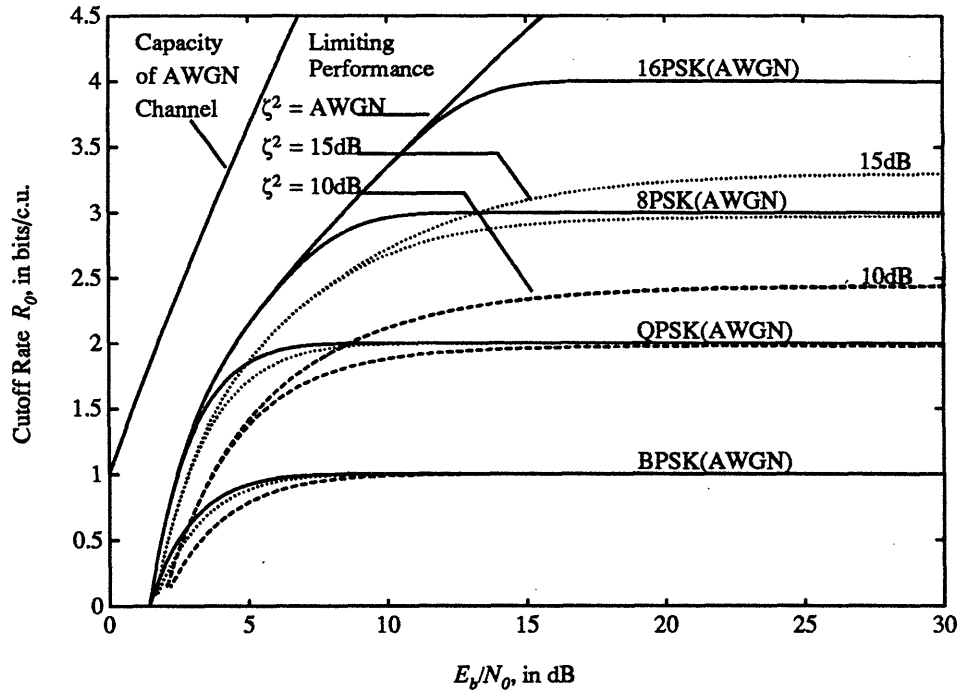

Figure 11
Behavior of Cutoff Rate $R_{0,1}$ Performance for MPSK Signaling on the Rician Channel With No CSI and Ideal Interleaving/Deinterleaving on a Symbol Basis ($N = 1$). The Limiting Cutoff Rate Performances are also Provided.

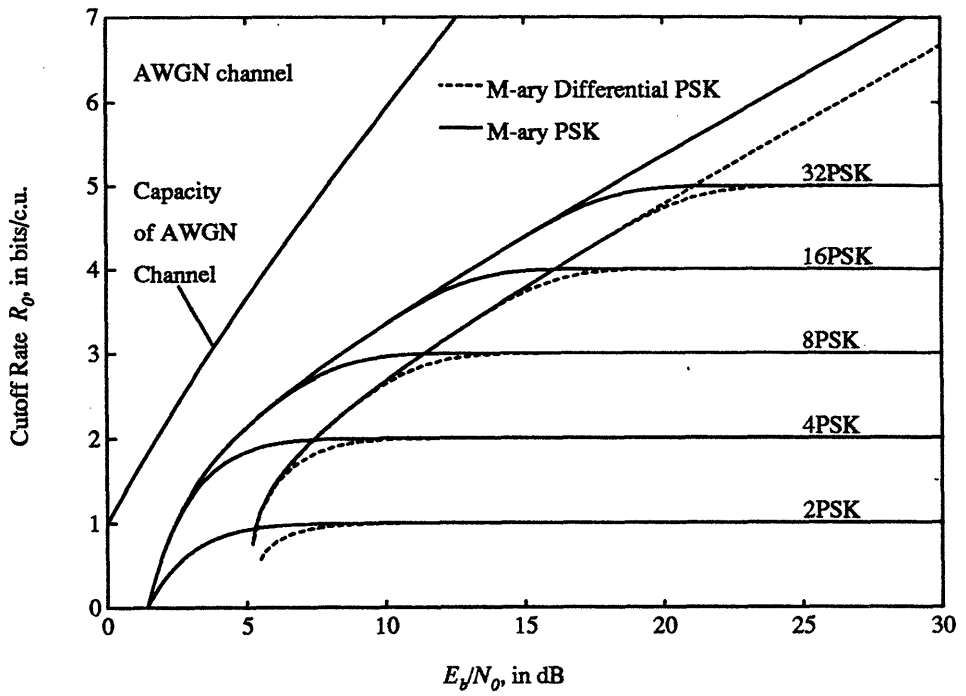

Figure 12
Comparison of R_0 Performance for MPSK and MDPSK on the AWGN channel.

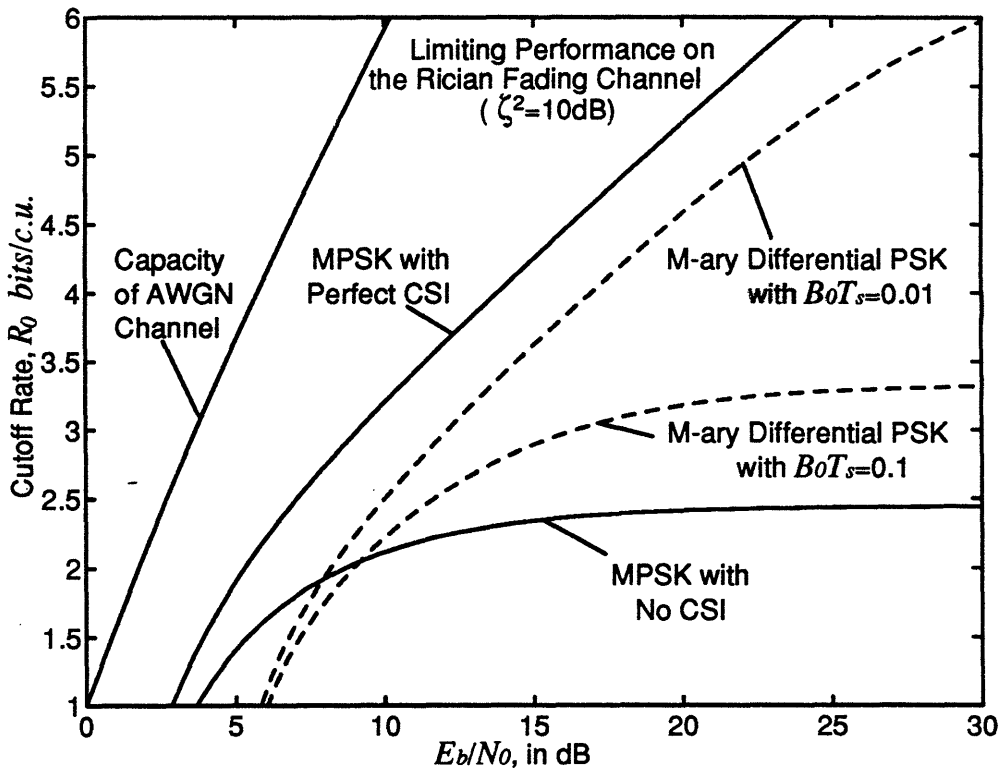

Figure 13
Limiting Performance of $R_{0,1}$ for MPSK Signaling with *Perfect* and *No* CSI and $R'_{0,1}$ for MDPSK with *No* CSI on the Rician Channel ($\zeta^2 = 10$dB) when *Ideal* Interleaving/Deinterleaving on a Symbol Basis ($N = 1$) is Employed.

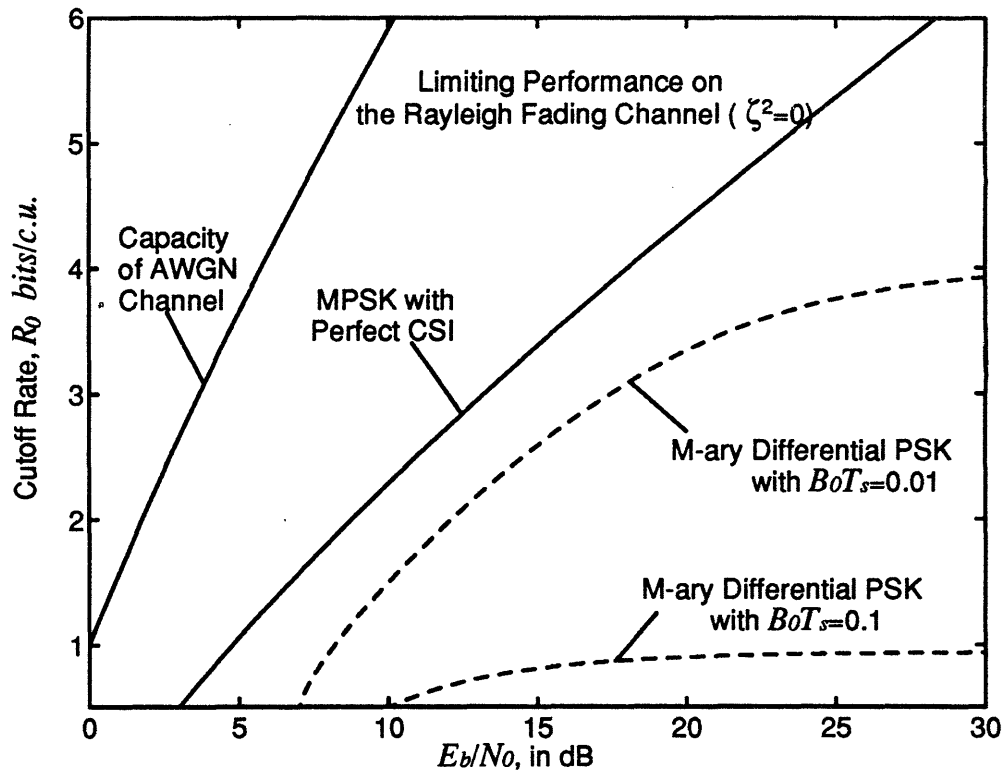

Figure 14
Limiting Performance of $R_{0,1}$ for MPSK Signaling with *Perfect* CSI
and $R'_{0,1}$ for MDPSK with *No* CSI on the Rayleigh Channel ($\zeta^2 = 0$)
when *Ideal* Interleaving/Deinterleaving on a Symbol Basis ($N = 1$) is Employed.